Radiocarbon dating

Irka Hajdas[1*], Philippa Ascough[2], Mark H. Garnett[2], Stewart J. Fallon[3], Charlotte L. Pearson[4, 5, 6], Gianluca Quarta[7], Kirsty L. Spalding[8], Haruka Yamaguchi[9], Minoru Yoneda[9,10]

[1]Laboratory of Ion Beam Physics, ETHZ, Zurich, Switzerland

[2] NEIF Radiocarbon Laboratory, Scottish Universities Environmental Research Centre, East Kilbride, Scotland, United Kingdom

[3]Radiocarbon Laboratory, Research School of Earth Sciences, The Australian National University, Canberra, Australia

[4]Laboratory of Tree-Ring Research, University of Arizona, Tucson, Arizona, USA

[5]School of Anthropology, University of Arizona, Tucson, Arizona, USA

[6]Department of Geosciences, University of Arizona, Tucson, Arizona, USA

[7]CEDAD-Centre for Applied Physics, Dating and Diagnostics, Department of Mathematics and Physics "Ennio de Giorgi", University of Salento, Lecce, Italy and INFN (National Institute for Nuclear Physics)-Lecce Section

[8]Cell and Molecular Biology, Karolinska Institutet, Stockholm, Sweden

[9]Department of Integrated Biosciences, Graduate School of Frontier Sciences, The University of Tokyo, Chiba, Japan

[10]The University Museum, The University of Tokyo, Tokyo, Japan

Abstract

Radiocarbon dating uses the decay of a radioactive isotope of carbon (^{14}C) to measure time and date objects containing carbon-bearing material. With a half-life of 5,700 ± 30 years, detection of ^{14}C is a useful tool for determining the age of a specimen formed over the last 55,000 years. In this Primer, we outline key advances in ^{14}C measurement and instrument capacity, as well as optimal sample selection and preparation. We discuss data processing,

carbon reservoir age correction, calibration and statistical analyses. We then outline examples of radiocarbon dating across a range of applications, from anthropology and paleoclimatology to forensics and medical science. Reproducibility and minimum reporting standards are discussed along with potential issues related to accuracy and sensitivity. Finally, we look forward to the adoption of radiocarbon dating in various fields of research thanks to continued instrument improvement.

[H1] Introduction

Radiocarbon (^{14}C) is a radioactive isotope of carbon produced naturally in the atmosphere by secondary cosmic rays. The discovery of ^{14}C and the establishment of the current method for radiocarbon dating came as a result of multidisciplinary efforts in the 20th century (Supplementary Figure 1). Shortly after the discovery of the ^{14}C isotope by Ruben and Kamen[1], minute amounts of ^{14}C were detected in nature[2-4], which triggered the development of a chronometer based on ^{14}C radioactive decay[3,4] (Figure 1). Produced in the atmosphere, radiocarbon is oxidized first to ^{14}CO and later on to $^{14}CO_2$ before entering the global carbon cycle **[G]**[5]. The ^{14}C content in the atmosphere is low ($^{14}C/^{12}C$ is approximately 10^{-12}), which is reflected in the biosphere and other carbon reservoirs, including the ocean and land. Once fixed in the matrix of organic matter — in plant tissues via photosynthesis and animal tissues via the food chain — ^{14}C concentration remains in equilibrium with the environment for as long as the host is alive. Death, closure of annual tree-rings or formation of cellular DNA, prevents cells from exchanging with new refreshed ^{14}C pool, thereby starting the radiocarbon clock (t_0). As the original ^{14}C content (A_0) decays with a half-life of 5,700 ± 30 years, the remaining ^{14}C content (A) provides a measure of time elapsed from t_0. The standardized procedure for reporting radiocarbon ages is shown in BOX 1.

The method's immediate use and success resulted from a combination of two key characteristics. First, as a naturally occurring radioactive isotope of carbon, ^{14}C is built into all carbon-bearing material (organic and inorganic) as part of the global carbon cycle. Second, a long half-life[6,7] enables ^{14}C to be used in a broad spectrum of applications and dating material formed over the last 55,000 years.

During the seven decades over which the radiocarbon dating method has been developed, significant technical and methodological refinements have occurred. These include ongoing efforts to construct, maintain and improve universal radiocarbon calibration curves **[G]** for the Northern[8] and Southern[9] hemispheres and the ocean[10], as well as notable instrumental developments. In 1977, the invention of the accelerator mass spectrometry (AMS) as an alternative to counting ^{14}C reduced the amount of carbon required for analysis from 1 g to 1 mg and decreased analysis time from days to 30 minutes for the equivalent precision. Moreover, during the last 2 decades, lower limit of carbon needed for AMS analysis was pushed to micrograms[11-14].

The downscaling of the required sample size has opened the gate for a whole suite of new applications. The potential of radiocarbon dating, previously most used in archeology and paleo-environmental science, has rapidly expanded across other fields such as biomedicine and art. Moreover, traditional applications have expanded to explore new materials (or conventional materials in new ways), facilitated by the smaller sample size requirements. An example of such cutting-edge applications is the use of the anthropogenic signal of nuclear testing, known as the ^{14}C bomb peak. The bomb peak is an excellent time marker for studying samples associated with biomedicine, forensics and environmental studies. Indeed a successful extension of radiocarbon-based biomarker research marked the transition to the 21st century[15] and compound-specific radiocarbon analysis (CSRA) has facilitated the tracing of carbon sources in the environment in finer detail than previously possible. Overall, ^{14}C is now used in a highly diverse array of applications ranging from dating DNA to solar activity reconstruction. This Primer introduces the radiocarbon dating method, its underlying principles, methodologies, and limitations. It also provides a wide range of examples of how AMS-based radiocarbon dating can be used as a tool to answer numerous research questions.

[H1] Experimentation

This section describes the process of selecting suitable material for radiocarbon dating and the necessary experimental steps. The potential archives of carbon and datable material are described, as is the choice of suitable material from these archives and the appropriate procedures for pre-analysis and purification. All of these considerations are crucial for successful radiocarbon dating. The normalized fraction of ^{14}C ($F^{14}C$)[16] is determined by either

counting (beta-ionization) or using AMS analysis (the main focus of this article). Based on the measured $F^{14}C$, the radiocarbon age is calculated and calibrated for chronological applications or assessed relative to relevant environmental changes in ^{14}C concentration (via $\Delta^{14}C$)[17-21]. The choice of material, requirements and corrections vary based in different research problems.

[H2] Equipment

[H3] Beta-counting techniques

The counting of electrons, which are the products of the beta decay of ^{14}C, evolved from the first Libby screen counters[22] to gas proportional counters (GPC)[23] and liquid scintillation counters (LSC)[24]. GPCs operate either on CO_2 or methane, where the beta particles are detected after they ionize the gas, filling the detectors. LSCs usually require samples to be converted to benzene (C_6H_6), which is then mixed with a scintillation agent such as butyl PBD. The beta particles resulting from the decay of ^{14}C present in the sample create scintillation within the mixture which can be detected and measured.

The development of the counters involved the reduction of background caused by impurities in material and cosmic rays[25]. The technique was well established by the mid-1980s with modifications to improve efficiency and sensitivity[26,27]. Both types of counters require larger samples and longer measurement times compared to AMS. However, numerous radiocarbon laboratories worldwide are still equipped with counters for processing relatively large samples, although often they also have graphite preparation lines[28] to enable analysis of smaller samples using AMS, i.e., these laboratories function as AMS satellite laboratories. Nuclear waste[29] and environmental monitoring[30] and the authentication of natural products[31] often rely on beta-ionization counting techniques because the costs of equipment/analysis are significantly lower and sample size is not a limitation.

[H3] Accelerator mass spectrometry

Since direct detection of ^{14}C using particle accelerators was demonstrated in 1977 [32-34], AMS has emerged as the most commonly used technique in ^{14}C analysis. In AMS, the direct measurement of the $^{14}C/^{13}C$ or $^{14}C/^{12}C$ ratio in the sample results in much shorter measurement times — from days to tens of minutes — and reduced sample material requirements — from grams to micrograms of carbon. AMS instruments are designed to extract carbon ions from a processed sample of graphite or CO_2, analyzing the extracted ion beam as it is passed through various

filters to remove unwanted and interfering species. While switching in a fast sequence between carbon isotopes, they detect and measure both stable and radioactive carbon isotopes (Figure 2)[35].

The ion source of the AMS system forms the first filter because it produces negative ions from graphite or CO_2. This is crucial for ^{14}C detection by AMS since it removes ^{14}N, which is the most abundant isobar **[G]** of ^{14}C, but which does not form negatively charged ions by sputtering. Negatively charged ions of ^{14}C are then transported through the rest of the system, which comprises two mass spectrometers, located at the low and high energy ends of a high voltage stage (Figure 2). Along each spectrometer, different dispersive elements are used as filters to select ions depending on their charge, mass and energy. To remove unwanted molecule species such as $^{12}CH_2$ or $^{13}CH_1$, the ions that passed the first spectrometer will interact with the so-called stripper medium (such as argon or helium gas) located at the high voltage stage. Here, electrons are removed, and molecular bonds are destroyed resulting in atomic ions in a positively charge state. They are mass filtered a second time in the mass spectrometer at the high energy end. Finally, the ^{14}C atoms and currents of ^{12}C and ^{13}C are detected. The measurement is executed relative to standards in order to derive absolute isotope ratios.

In recent years, AMS has undergone further technical developments, resulting in the detection of ^{14}C at much lower energies than before, which requires much lower terminal voltage[36-38]. This has led to the downscaling of AMS instruments and facilitated more reliable and stable operations in AMS laboratories, which are closely comparable to conventional mass spectrometry laboratories[39,40]. Further improvements are related to the set-up of gas-accepting ion sources for the analysis of microgram samples[12,41-43] and direct analysis on CO_2 resulting from the combustion in Elemental Analyzer[44], wet oxidation[45], acid hydrolyses[46] or laser ablation (LA-AMS)[47] and the use of systems based on positive ions [48].

[H2] Sample Material

Radiocarbon dating can only be applied to samples that contain organic or inorganic carbon. Material older than 55,000 years old is beyond the limit of radiocarbon dating, as determined by the Libby half-life.

[H3] Natural archives

A broad spectrum of material from various terrestrial and aquatic environments is suitable for radiocarbon dating (Supplementary Table 2). Material from terrestrial archives **[G]** such as wood and remains of terrestrial plants and animals typically contain direct records of atmospheric ^{14}C present in CO_2, fixed into terrestrial plant tissues or indirectly into animal tissues via the food chain. There are a few exceptions: when a localized source of ancient CO_2 is present, such as in a volcanic vent or when the food chain is dominated by a ^{14}C reservoir effect**[G]**. Reservoir effects occur typically in freshwater aquatic or marine systems, when the carbon in tissues of organisms or inorganic deposits reflect the presence of older carbon within marine circulation systems or within ground water enriched with old geological carbonates (^{14}C-free). This can skew radiocarbon dating results erroneously by several hundred years compared to the contemporary terrestrial and atmospheric records. In such circumstances, dating for a range of plants, shells, corals and sediments must be corrected to enable accurate dating. Similarly, soil, sediment and speleothem **[G]** samples can have a range of other more complex sources of carbon originating from old limestone rock or old organic carbon stored in soils, and thus require modeling and correction to improve the ^{14}C dating accuracy. Anthropogenic products such as art and items of everyday life can also have a more complex carbon footprint through which radiocarbon dating can unravel sources and track down counterfeits.

[H3] Choosing optimal samples

The success of any study using radiocarbon dating is dependent on the materials selected and how they are sampled. Research questions should be formulated prior to sampling, most notably to define the expected outputs and possible limitations to dating precision and accuracy. For example, dating precision in some periods is severely limited by the shape of the radiocarbon calibration curve (Figure 3), and this should be considered ahead of sampling in applications such as archeology [49,50] or the study of artworks[51] where precision dating is paramount. Depending on the objective of the dating study (for example, determining the date of an event, artefact or proxy record), there may be a variety of options for carbon samples; in such cases, it is essential to prioritize the material most appropriate to best answer the research question.

Sample size is important, and must be optimized to ensure the success of radiocarbon dating, but prevent any unnecessary damage of the artefact. Another critical step is to identify

potential carbon sources within the selected material (considering the previously described reservoir or carbon cycle-related effects). A crucial part of this exercise is the possibility for contaminating carbon to have been added to the sample prior to recovery.

Contamination can be due to natural processes such as incorporation of exogenous carbon by, for example, bone deposited in soils or by conservation of bone with polymers or glue. It is also essential to consider how closely the true age of the carbon in the sample — for example, pre-aged coffin wood made from a center of a large oak trunk — reflects the date of the event of interest, like date of burial)[52]. A single charred seed in an archaeological sample should not be used for radiocarbon dating, as it may be intrusive or residual from bioturbation and post-deposition processes. Rather, a cluster of seeds found as part of a dating assemblage is preferred[53]. Other potential contaminants include modern roots in archaeological contexts or varnish on paintings, and must be avoided or accounted for in the sampling protocol, by using a higher mass of bulk sediment or sampling the canvas of a painting.

[H2] Sample preparation

Most samples used in radiocarbon dating will require a sequence of preparation steps, often involving both physical and chemical processing of the sample (BOX 2). The aim of all of these steps is to remove contamination and to convert the sample into a pure and condensed carbon form such as graphite or CO_2, which is suitable for AMS analysis. For conventional ^{14}C measurements using beta-counters, CO_2 and methane or benzene are the dominant form for GPC or LSC counters, respectively. The first step is designed to separate only carbon relating to the specific deposit of interest (for example a grave or a fireplace), in the case of ^{14}C applications as a chronometer, or only carbon relating to the source of interest in the case of applications using ^{14}C for carbon source apportionment, fluxes or turnover times.

[H3] Physical processing

Physical preparation of samples includes visual and microscopic examination. This is performed to verify that the physical sample type and composition are as expected, and are suitable for measurement. Some samples such as wood can be quite straightforward to clean and prepare. However, waterlogged wood has little or no preserved cellulose,

potentially making the separation of sufficient carbon difficult. Bones may have been poorly preserved, hindering the separation of collagen needed for radiocarbon dating.

Physical pre-screening is also used to determine the mass of the sample, and to assess the likelihood that the sample will withstand the planned pretreatment procedure. Physical preparation can also include removal of visually identifiable exogenous carbon such as roots, and mechanical treatment such as crushing, cutting or grinding. The latter steps facilitate subsequent chemical treatment, by for example increasing surface area or homogenizing material.

[H3] Chemical processing

An assessment of the chemical composition of a sample can predict how it will behave during processing, whether treatment is likely to be successful and to identify chemical contaminants that must be removed prior to measurement. This is particularly helpful if these factors are uncertain or if little information is known about the sample. Elemental analysis provides information of %Nitrogen and %Carbon preserved in a bone, for example[54]. Fourier Transform Infra-Red Spectroscopy (FTIR) is very helpful in this regard and can be performed without loss of sample material[55-60]. Chemical pretreatment of the sample material may either remove contamination with carbonates using acid such as solution of hydrochloric acid when looking at soil organic carbon, for example[61,62], and/or isolate a particular chemical fraction from a complex mixture known to be less prone to contamination than other components, such as is the case when isolating collagen from a whole bone. Separation of carbon inherent to the sample material may also be facilitated by the measurement of specific compounds or classes of compounds of interest from a larger chemical mixture, such as n-alkanes from lake sediments. An extensive range of pre-treatment approaches has been developed[15,63-66].

[H2] Standards and processing blanks

Samples of known age (secondary NIST standard HOx2 [19,67] are used for normalization. Secondary standards provided by International Atomic Energy Agency (IAEA)[68] are prepared alongside unknown materials as targets for AMS analysis as graphite or CO_2, or as CO_2 or methane in GPC[23] and benzene in LSC [24,25]. Standards are also used to monitor contamination introduced during processing. Modern contamination is detected using ^{14}C-free material older

than 100,000 years, often termed blanks or background standards. Detection of old carbon contamination is tested against modern references. The material used as standards in radiocarbon dating laboratories includes international standards such as those produced by NIST and substances used in International Radiocarbon Intercomparison series [69]. Laboratories may also use in-house standards prepared from suitable sources of material, such as dendrochronologically dated wood.

Processing blanks are material-specific and pretreatment-specific, and accompany sample preparation of the same type and size to monitor contamination with exogenous carbon. For example, charcoal can be prepared using an Acid-Base-Acid (ABA) treatment (also known as AAA for Acid-Alkali-Acid), and wood can be prepared by separation of alpha-cellulose (BOX 2). Other organic materials such as bone and peat also require different pre-treatment strategies. Carbonates require different processing, therefore ^{14}C-free carbonates such marble (IAEA C-1) and interglacial shells, corals and stalactites are used as processing blanks.

[H2] Data collection

Each AMS facility has its own data collection system, with commercially built instrumentation equipped with a database to store information about the samples and their measured radiocarbon ages. AMS analysis of a single sample is performed in multiple cycles, depending on the sample material and required precision. Each solid graphite sample can be measured in multiple runs, with the cumulative run-time ranging from 30 to 120 min. Measurement time for gas targets containing micrograms of carbon vary from few minutes up to a maximum of 10–12 minutes, depending on sample size. The counted ^{14}C atoms and currents of ^{12}C and ^{13}C are registered for each measurement cycle. Data evaluation processes are also a part of the measurement, allowing for simultaneous control of the analysis via remote and in-laboratory software. The final data evaluation is performed after the measurement is completed. In this step, stability and performance are assessed and required corrections are made.

[H2] Ethics considerations

Some radiocarbon dating applications require ethical considerations when sampling or even when deciding whether radiocarbon dating is appropriate. In biomedical applications, the collection, storage and processing of human biological material must follow ethical guidelines set by national authorities both where the samples are obtained and where they are processed.

While individual AMS facilities may not require ethical permits in order to receive and process such samples, it is the responsibility of the individual submitting the sample to have acquired all the necessary permissions for working with human material.

In applications related to the antiquities trade[70], to prevent radiocarbon dating of looted objects, most radiocarbon laboratories request documentation of an object's origin and ownership[71]. Ethical guidelines apply when art or artefacts of cultural and/or religious significance or when ancient living trees are sampled. Sampling of such items must be carefully planned to prevent unnecessary destruction and damage[72,73]. Sampling in different countries and transfer of sample material — such as removal of samples from Egypt — may be subject to special regulations and require special permissions. Therefore, the best practice is for international research projects to include collaborators from the country where research sites are located, which is of benefit to the project's outcome.

[H1] Results

The raw data obtained through radiocarbon measurements requires data processing. Analysis includes statistical analysis, age correction in order to obtain corrected and normalized values of sample ^{14}C content. Finally, calibration or Bayesian modelling is applied to obtain calendar ages.

The first step in the processing of radiocarbon dating data is to calculate the carbon isotopic ratios ($^{14}C/^{12}C$, $^{14}C/^{13}C$ and $^{13}C/^{12}C$) from measured quantities of ^{12}C, ^{13}C and ^{14}C. These data are then processed using different software depending on the class of instrument, the need for specific corrections, the level of precision required and the specific applications[74-77]. The measured $^{14}C/^{12}C$ ratios are normalized to a standard corrected for isotope fractionation ($\delta^{13}C$)[78] **[G]** and accelerator and sample processing backgrounds, then expressed in conventional units ($F^{14}C$) **)** (BOX 1). Conventionally, 95% of the ^{14}C content in 1950 CE of a particular batch of oxalic acid HOx1 (NIST) is used as a reference. Due to dwindling supplies of HOx1, a secondary standard HOx2 is now being used, with an activity ratio **[G]** of 1.2736 in relation to the original standard[67].

Correction for machine and sample processing backgrounds is performed by subtracting values obtained from ^{14}C-free materials that are either unprocessed —such as fossil graphite — or chemically processed in parallel with the samples — such as bones or wood older than the dating limit of ^{14}C — from the measured sample $^{14}C/^{12}C$ ratios. Processing blanks are critical

when dating samples older than 30,000 years because the blank correction of the measured value for such old samples ($F^{14}C$ <0.025) introduces a large uncertainty and becomes the limiting factor for ages close to the limit of the method. Measured $F^{14}C$ of samples older than 50,000–55,000 years is lower than 0.002 therefore of a similar level to blank samples. The effect of contamination is dependent on the $F^{14}C$ and the amount of the carbon added to samples in preparation. The constant mass contamination correction **[G]** is applied for low carbon masses that feature for very small samples (<0.1 mg of carbon)[44,79]. However, finite ages on samples as old as 50,000–55,000 years can be determined for samples of 1 mg of carbon.

[H2] Statistical analysis and error

Experimental error on the measured carbon ratio is calculated by considering both the Poisson statistics associated with ^{14}C counting and the scattering of the data obtained on the replicated analysis performed on each sample. One standard deviation uncertainty level of 0.3%, which represents ±20/30 years in the radiocarbon timescale, is routinely achieved on samples younger than 10,000 years (for example [80]). Overall uncertainty includes scatter due to sample-specific preparation, which is determined by preparing the same sample material — often of known age, such as tree-rings — multiple times[81]. For routine analysis a sample scatter multiplier or laboratory factor is applied. High precision analysis, desirable in some applications such as annually resolved tree-rings or art objects, requires multiple samples and coherent reading of the $F^{14}C$.

[H2] Reservoir age correction

For samples containing carbon from reservoirs other than the well-mixed atmosphere and terrestrial biosphere, the measured radiocarbon ages usually require correction before they can be placed on a common calendar timescale. This is achieved after all other corrections and calculations have been performed upon the measured sample $^{14}C/^{12}C$ ratio.

[H3] *Marine radiocarbon reservoir effect*

Correction of samples containing marine carbon accounts for the spatiotemporal variability of marine radiocarbon records and is expressed as the marine radiocarbon reservoir effect **[G]** (MRE)[10,82]. At any location, the MRE is the product of global scale mechanisms in marine environments, which include the extended residence of ^{14}C atoms in the marine reservoir once water is circulated away from the air-water interface at the ocean surface, and the rate of gas

329 transfer of CO_2 across this interface. Correcting for the MRE applies a value for the global
330 average ocean to the measured sample ^{14}C age[83]. The global MRE is expressed as the
331 difference in ^{14}C age between marine and atmospheric carbon, varying through time; this
332 correction should be derived from a separate international calibration curve for the global
333 marine reservoir, currently Marine20[10]. This calibration curve represents the marine reservoir
334 response to the fluctuations in $^{14}C/^{12}C$ through time in the atmospheric reservoir[83]. In addition
335 to use of a calibration curve for the global marine environment, any local variation from the
336 global average MRE must be calculated and applied to the samples in question. This local
337 difference from the global average MRE is known as ΔR and should always carry an associated
338 uncertainty[82]. Values for ΔR and its associated uncertainty are empirically derived, and a
339 researcher may evaluate ΔR themselves[84] or use established literature values, such as those
340 available in the Marine Reservoir Database[85]. Note that, with the advent of Marine20,
341 literature values of ΔR that were obtained using earlier versions of the atmospheric and
342 marine calibration curves must be recalculated with Marine20 before use because the new
343 Marine20 accounts for temporal changes in the globally averaged MRA[10].

344 [H3] *Freshwater radiocarbon reservoir effect*

345 While the global MRE and many local ΔR values are relatively well established, this is not the
346 case for the freshwater carbon reservoir. This is because the underlying mechanisms that
347 govern the existence and size of a freshwater radiocarbon reservoir effect **[G]** (FRE) are highly
348 location-specific. These generally involve variations in the input of geogenic, pre-aged or
349 radiocarbon-dead carbon to a freshwater system, and/or residence time of ^{14}C atoms in a
350 freshwater system, for example due to lake stratification[86]. In effect, the total organic carbon
351 of lakes within a carbonate rich catchment area or with regional volcanic CO_2 sources can yield
352 a depleted ^{14}C signal. If the presence or absence of a freshwater reservoir effect has not
353 previously been established for the system from which samples were obtained, efforts should
354 be made to do this, by comparing measured ^{14}C values with an independent age control, such
355 as contemporaneous terrestrial carbon, known ages for recently-fixed freshwater carbon or
356 other absolute age markers, including volcanic ash or varves, i.e., annual laminations in
357 sediment. A correction may then be made by subtracting the FRE in ^{14}C years from the
358 measured sample age. This approach assumes the size of the FRE is constant with time.
359 Changes in the nature of the mechanisms driving the size of an FRE can result in temporal FRE

fluctuations even within a small geographical area[87] therefore terrestrial organic matter is the first choice for radiocarbon analysis (Supplementary Table 2) and failing this, cross-checking results with other dating methods.

[H2] Approaching mixed reservoir samples

It is possible for samples to contain a mixture of carbon originating from two or more reservoirs. This typically occurs where a terrestrial animal consumes a proportion of marine and/or freshwater carbon as a dietary resource, in conjunction with dietary carbon obtained from the terrestrial biosphere. The most common examples of this are terrestrial omnivores, like humans and pigs; terrestrial carnivores like dogs and foxes can consume marine protein, and even terrestrial herbivores like sheep and deer may consume marine plants such as seaweed, if it is available and accessible. If a mixed-reservoir situation is suspected, a series of steps are important to account for this[88]. First, the source and quantity of non-terrestrial carbon should be identified. Stable isotopes of carbon, particularly when coupled with isotopic ratios of other elements like nitrogen and sulphur can be very helpful in distinguishing between isotopic signatures of different reservoirs in the sample, and they can establish the proportion of carbon from each reservoir[89-91]. Determining the carbon proportion from each reservoir can be achieved via mixing models, from simple linear regression[92] to Bayesian modelling[93]. Usually, the quantification of the proportion of non-atmospheric carbon also has an associated uncertainty, derived from factors such as variability in the isotopic composition of end-members for each reservoir, and in the analytical method used for quantification of non-atmospheric carbon[91,92]. It is important that this uncertainty is factored into any subsequent calibrations. Second, the radiocarbon reservoir effect of the non-atmospheric carbon must be established, along with the uncertainty of this value. Where the non-atmospheric reservoir is marine, the measured radiocarbon value for the sample can then be calibrated to a calendar timescale using a mixture of the atmospheric and marine curves.

[H2] Corrections for dead carbon fractions

Frequently carbonates precipitated in cave environments have a different ^{14}C signature than the atmosphere. This specific reservoir effect is called the dead carbon fraction **[G]** (DCF). It reflects a difference between atmospheric ^{14}C content and the signal recorded in carbonates at the time of their formation. The dissolved inorganic carbon (DIC) in water passing through soils has a mixed signal, where the dead carbon component of the (typically) limestone

bedrock fluctuates from site to site. For this reason, speleothems are complex carbon records. However, the possibility of precise uranium-thorium dating[94] and the extensive records represented in such archives around the globe offer the potential to utilize such material for extension of the radiocarbon calibration curve[94,95]. Moreover, recent high-resolution studies have demonstrated the potential of the DCF as a proxy of paleoclimate[96]. The new LA-AMS technique[47,97] allows time-effective sampling and measurements of continuous profiles of $F^{14}C$, which can be a useful pre-screening tool in environmental studies of the last 100 years.

[H2] Calibration

Atmospheric ^{14}C has been impacted by a range of natural (solar, geomagnetic, global carbon cycle) and anthropogenic (bomb testing, fossil fuels) factors, introducing considerable variability in ^{14}C through time (Box 3) .If ^{14}C concentrations in the atmosphere remained constant through time the measured radiocarbon age — expressed in ^{14}C years Before Present (BP) — would not require calibration. Moreover, calibration compensates the offset caused by the use of the wrong Libby half-life (Figure 1, BOX 1, Supplementary Table 1). Radiocarbon age must be calibrated to a curve based on measurements of ^{14}C from samples of known age appropriate to the sampling location — whether that is the Northern or Southern hemispheres, or a marine environment, for example. The calibrated radiocarbon age is referred to as calendar ages counted backwards from 1950 CE (cal BP) or to calendar years before and within Common Era (BCE/CE). The IntCal radiocarbon calibration curves[8,9] are a community resource constructed from measurements of ^{14}C made in different laboratories on a range of securely dated samples. The recently updated compilation of data was published in 2020[8]. For the past 13,900 years (from 1950 CE back to 13,900 cal BP) calendar dated tree-rings are used to produce calibration curves. Beyond this, back to around 55,000 years ago, a range of other measurements from highly resolved lake and marine sediments, speleothems, corals and non-calendar secured tree-rings are statistically integrated to create the most accurate representation of past atmospheric ^{14}C currently possible (Figure 3a). The accuracy of any calibrated date is limited by the precision of the radiocarbon dating and the calibration data available, and by the natural variations in ^{14}C over time (Figure 3b and 3c).

The calibration is the last step in radiocarbon dating of the sample. The measured $F^{14}C$ values or radiocarbon age are calibrated using the most updated calibration curves (Figure 4a). The

IntCal data are available online and are an integral part of freely available calibration software[98,99].

The years after 1950 correspond to the post-nuclear testing era. Atmospheric ^{14}C concentrations measured in CO_2 of air or dated tree-rings including some of tropical species[100] display what is known as the bomb peak. The bomb peak has other implications and uses for dating of post-1950 material (BOX 4). Higher than the natural ^{14}C concentrations of the bomb peak period (1953 until now) can be easily detected in samples formed less than 70 years ago ($F^{14}C$ >1). The measured value is then calibrated using compiled bomb peak data[101] (Figure 4b) and updated data sets at the CALIBomb web page.

[H2] Bayesian Modelling

The proper analysis and interpretation of radiocarbon data requires a robust statistical framework facilitating the calibration of conventional radiocarbon ages which typically do not produce normally distributed calendar time ranges, the interpretation of large sets of measurements and the combination of relative and/or absolute chronological information. This framework has been widely developed by using a Bayesian approach[102,103].

In typical chronological applications this theorem[104] can be used to combine absolute, calibrated radiocarbon ages — likelihoods — with independently available information about the chronology — priors — in order to calculate a refined chronological model — the posterior (Figure 5). The prior information can be either calendar or relative. Examples of prior calendar information include when we know that an event has occurred in a certain time period or range, or after or before a certain date. Relative prior information includes when the order of a series of events is known. There are, of course, different possible situations to be considered. For example, a Bayesian model of a sequence of samples from a sedimentary record or a series of ^{14}C dated tree-rings has a potential to improve the precision of calibrated ages[103,105].

Other models include the stratigraphic order as prior information, and allow for coeval events to be chronologically grouped. This is for instance the case with sedimentary sequences when we know that a set of samples belongs to the same event — for instance a precise climatic event or a flooding, or in the case of an archaeological stratigraphy, an event like a destruction layer or a fire event or to the same cultural horizon[49]. The set-up of a proper and correct prior chronological model and its formalization in mathematical terms is a critical step in Bayesian

analysis of radiocarbon ages. It requires combination of available information such as series of events including different, properly bounded phases[106]. Bayesian advanced statistical tools are included in dedicated routines available in different calibration software such as OxCal[103,107], BCal[108], MatCal[109], ChronoModel[110].

[H1] Applications

Radiocarbon analysis is a powerful tool employed in studies of human and earth history of the last 55,000 years. The examples presented here include anthropology and archaeology, paleoclimatic research, terrestrial and oceanic environmental studies, biomedicine, cultural heritage, art research and forensic science. The list is much longer and expanding continuously with the development of new interdisciplinary applications. The main benefits from the close collaboration across the fields is becoming evident as the new radiocarbon dating tools are applied to answer questions formulated prior to the field work and sampling.

[H2] Anthropology and archaeology

Radiocarbon dating in archaeology and anthropological studies is not simply used to calculate the time that has elapsed from a past event[111]. It has become a powerful and invaluable tool for extracting new information about human activity, which would be unattainable with relative age alone, such as contemporaneity, rate of change and the spatial range and diffusion of events[112] that can also be interpreted in the context of parallel paleoclimatic data such as ice core records.

Advances in isolation and purification techniques also have a considerable effect on quality control, which is a critical issue in this area as it deals with samples susceptible to diagenesis **[G]** and contamination[113,114]. Ultrafiltration to remove lower molecular weight fractions has been used to purify gelatin extracted from bones [115]. AMS can now measure samples with carbon content as low as tens of micrograms[11-14], allowing for sampling of extremely precious fossil bones[116-118] and facilitating radiocarbon dating and DNA analysis on the same bone. Another purification technique based on density separation using heavy liquids, known as carbonate density separation allows for the separation of calcite and aragonite**.** The separation of calcite is used for dating mollusk shells (which are involved in a range of archeological contexts), resulting in improved accuracy of radiocarbon ages of shells older than 30,000 years[119]. Compound-specific radiocarbon analysis **[G]** (CSRA) has also been successful at removing contaminants[120,121]. Using CSRA, a single amino acid found almost

exclusively in mammalian collagen — hydroxyproline — was isolated and measured by AMS. All these refined methods of separation carbon inherent to the bones or shells have been used in revising the chronologies of Middle and Upper Paleolithic archeological sites[122-124], which is essential in the debate surrounding the co-existence between Neanderthals and anatomically modern humans and the extinction of the Neanderthals. CSRA has also been used in dating remains of food processed and stored in archaeological pottery using biomarkers[125,126]. Measurements such as these provide stronger ties to human activities and increase the archaeological implications of the radiocarbon dating.

In the search of datable material phytolith **[G]** occluded carbon has been considered. For example, rice phytoliths in China's Lower Yangtze region, which has been recognized as one of the earliest examples of rice cultivation, were dated to 9,000-9,400 cal BP along with other material from the same layer or context [127]. However, some other studies using radiocarbon dating of phytoliths have shown inconsistent ages [128,129], which triggered research into the carbon sources and treatment methods for phytoliths, and indicated potential contribution of old soil carbon[130].

The use of radiocarbon dates in conjunction with other chemical and statistical analyses and spatial and archaeological datasets has been a major driving force in estimating human migration and population history. The progress of DNA analyses and ZooMS (mass spectrometry for zooarchaeology) have facilitated the determination of biological ancestry or the detailed taxon of samples lacking morphological information which can be combined with their radiocarbon dates[131,132].

Bayesian modeling for the calibration of radiocarbon data has been useful in tackling uncertainties in archaeological periodisation[133] when radiocarbon dates and their probability distributions are used as a proxy for estimating prehistoric population[133,134]. If care is taken to collect accurate spatial data for each material sampled for radiocarbon dating, the formation history of archaeological sites and larger context human migration and population histories may be revealed. Examples range from dating an early human occupation in Boomplaas Cave, South Africa[135] to chronology of the earliest occupation at the Neolithic site Çatalhöyük in central Turkey[136]. Close collaboration between radiocarbon dating researchers and on-site archaeologists is beneficial in order to date samples most representative of the archaeological event of interest. Such co-operation combined with statistical analyses quantifying

probabilities and uncertainties (see for example[137]) is expected to address previously unanswerable archaeological questions.

[H2] Paleoclimatic research

Paleo-environmental archives of the last 55,000 years are often dated by radiocarbon dating[21] (Figure 6). Among the records are peat sequences[138], bogs[139], lake sediments[105,140], marine sediments[141,142], fossil trees[143], corals[144,145], speleothems[146-148], paleo soil[149] and loess[150,151]. Radiocarbon dating assists in pinpointing climatic and environmental shifts observed as shifts in various proxy data **[G]** such as pollen spectra or stable isotopes by dating the corresponding natural archives. For example, ice rafted debris identified in the North Atlantic sediment cores — a result of Heinrich Events — were accompanied by foraminifera shells, which were radiocarbon dated[152]. These radiocarbon ages of foraminifera were used to build a chronology for climatic events associated with Heinrich Events, which facilitated global climatic correlations[153,154]. Global or regional correlations depend on chronology and time markers. Thus, application of radiocarbon dating is frequently accompanied with the use of other dating techniques such as dendrochronology, optically-stimulated luminescence, uranium-thorium dating, lead-210 dating, varve counting or tephrochronology. The combinations of methods can be used to date volcanic eruptions[155-158], landslides[159-161], earthquakes[162,163], tsunamis[164,165] and floods[166,167].

While the tree-ring record can date a range of extreme events for specific geographic regions across the last 14,000 years, older events and many temporal and regional gaps in the tree-ring record mean that there are numerous tree-ring applications also relying on radiocarbon dating[167,168]. Variable atmospheric radiocarbon can be due to changes in production rate (BOX 3) and measurements of annual, calendar dated tree-rings have also shown rapid ^{14}C production in the atmopshere**.** These are known as Miyake events after[169] and have documented ^{14}C production increases of >1% over a ~1 year timespan. Miyake et al., [170] suggested that such a rise in atmospheric ^{14}C concentration might be due to solar energic particle **[G]** events. Additional rapid events over the Holocene have been identified at 775 CE, 993 CE, 660 before CE (BCE) and 5480 BCE, and documented across the globe[169,171-174]. These rapid excursions have provided a unique opportunity to aid in radiocarbon calibration and high precision dating[175-177].

Radiocarbon also provides insight into the Earth's magnetic field. Variations in the Earth's magnetic field cause fluctuations in the number of cosmic rays entering the Earth's atmosphere and therefore directly influence the production of ^{14}C. Radiocarbon calibration curves like IntCal13 and IntCal20 have documented changes in ^{14}C production over the past 55,000 years including several large production events at 41,000 years (Laschamp) and 35,000 years (Mono Lake) events[8,178]. These radiocarbon production records closely match geomagnetic field reconstructions based on paleomagnetic data detailing the strong relationship between them[179] and opening up new applications.

Radiocarbon dating of megafaunal remains is a robust method to determine extinction times. Causes of megafaunal extinctions usually fall into two categories: climate change and human hunting. Radiocarbon has provided clear dating of extinctions, for example the extinction of giant deer[180] and giant rhinoceros[181] or megafauna in Siberia [182]. However, some dating of megafauna extinction is near the limit of radiocarbon, as in the case of Australian megafauna, making causes difficult to infer [183-185]. New Bayesian modelling methods like radiocarbon-dated-event counting coupled with climate information and human population densities are making strides in determining causation of extinctions [186]. In this example megafauna decline corresponded to global temperature decreases but not with human population [186]. Future studies will need to employ these more sophisticated models to determine causation and relationships of megafauna extinctions.

[H2] Atmosphere

Production of radiocarbon takes place continuously in the atmosphere therefore understanding atmospheric $^{14}C/^{12}C$ variability past and present is central to the radiocarbon dating of any material. Anthropogenic effects caused by fossil fuel emissions and excess of artificially produced ^{14}C like with nuclear technology have a profound impact on the atmospheric ^{14}C content (BOX 3). The first measurements of atmospheric $^{14}CO_2$ were initiated in Wellington, New Zealand in 1954, and a few years later in the Northern Hemisphere (for summary and overview see[187-189]) following the rise of the ^{14}C bomb peak[101,190] (BOX 4). Perturbations of the natural atmospheric ^{14}C reservoir provide an excellent tracer for studies of the atmospheric circulation[191] and of the carbon cycle[192]. The record is extended by the measurements of bomb peak ^{14}C in tree-rings[193,194], allowing for more detailed studies of regional and seasonal differences caused by the location of the Interhemispheric Convergence

Zone (ITCZ)[191,195]. Combined atmospheric and ocean observations of the ^{14}C bomb peak evolution provide information on the uptake of anthropogenic CO_2 emissions by the ocean[196] and modeling of future atmospheric ^{14}C content[197]. Radiocarbon analysis is a crucial tool for qualitative estimations of fossil fuel emissions in urban regions [198-201].

In addition to gaseous emissions, combustion processes coming from power plants, fires and engines contribute particulate matter to air pollution. These carbonaceous aerosols are composed of light-scattering organic carbon and light-absorbing elemental carbon, also known as black carbon. Measuring the isotopic composition of carbon (^{14}C and stable isotopes $\delta^{13}C$) of aerosols is used to quantify and identify sources of aerosols, whether they are from organic or elemental carbon fractions[202-204].^{14}C emissions from the nuclear power plants can be detected in gaseous forms and aerosols[205,206] as well as in vegetation[207] and as a part of nuclear power plant monitoring procedures.

[H2] Terrestrial environment

Radiocarbon measurements used to create a chronological framework for studies reconstructing the past environment — such as changes in vegetation distributions and climate — usually rely on the availability of suitable depositional archives containing chronologically stratified layers, for example from peats and lake sediments. In soils, processes inherent to the formation of these matrices, such as mixing from bioturbation, and the continual addition of de novo carbon from living vegetation, normally prevents the establishment of a radiocarbon age for the soil in the conventional sense. Instead, ^{14}C measurements of soil reflect the rate of turnover of soil carbon over decadal-to-millennial timescales, providing crucial information for modelling terrestrial carbon cycling[208,209]. This has proven particularly valuable during the post-bomb era, where the transient enrichment of soil carbon with bomb peak ^{14}C has been traced to provide high resolution estimates of carbon turnover. Recognizing that soil is a complex mix of many different components, recent developments in this area have focused on isolating fractions to determine the rate at which they are cycled. Examples include chemical and density separation[210], CSRA[211] and ramped oxidation-pyrolysis[212]. Radiocarbon measurements on charcoal and/or biochar have also been used to address the role of black or pyrogenic carbon in the long-term carbon storage and/or turnover of soils[213,214].

Over recent decades, radiocarbon analysis has been increasingly used to trace the products of soil decomposition, through analysis of soil-respired CO_2, methane, dissolved organic carbon (DOC) and particulate organic carbon (POC). Much of this work depends on the concept that disturbed systems will release older carbon than they would otherwise, resulting in the reintroduction of carbon that effectively had been locked away into the contemporary carbon cycle. For instance, concern that melting permafrost in high latitudes is releasing old carbon and contributing to rising atmospheric CO_2 concentrations — known as the permafrost carbon feedback — has driven a wave of ^{14}C measurements in this area of high carbon storage[215]. Similar radiocarbon approaches have addressed the effects of anthropogenic land-use change on the release of old carbon, such as drainage and deforestation of tropical peatlands[216].

Radiocarbon measurements, often in conjunction with stable carbon isotope analyses, can unravel the contribution of different sources to various carbon pools. Since ^{14}C is absent in fossil carbon due to its immense age, ^{14}C measurements can be used to quantify the contributions of anthropogenic emissions to atmospheric CO_2 and methane [200,217]. Similarly, the ^{14}C concentration of aquatic DIC can help partition its sources between ancient geological and younger organic components such as plants and the result of soil respiration, and to determine residence times in groundwaters[218]. ^{14}C analysis has been used to identify the carbon used by organisms to better understand their functioning. For example, ^{14}C analysis of fungal fruiting bodies[219] has been used to determine whether a fungal species is mycorrhizal **[G]** or saprotrophic **[G]** and, through ^{14}C analysis of respired CO_2, show that a particular saprotrophic fungi used soil carbon that is up to 1,200 years old[220]. Radiocarbon analysis of soil and freshwater fauna has also been used to infer feeding behaviour[221,222].

Another major role in environmental applications for radiocarbon is in characterizing the source of carbon sequestered into carbonate minerals. Carbonate mineral sequestration is a natural method of removing CO_2 from the atmosphere and storing it into carbonate minerals. It is one of the many components being trialled to reduce atmospheric CO_2. Radiocarbon dating can determine whether the carbon in the newly formed minerals is from the contemporary atmosphere or is old recycled carbon, which is crucial for lowering atmospheric CO_2 content [223-225].

[H2] Ocean environment

Radiocarbon can enter the ocean in particulate form, from rivers and dust, or through air-sea gas exchange of CO_2, becoming part of the oceans' carbon pool. Air-sea gas exchange of $^{14}CO_2$ does not occur uniformly across the ocean, factors such as temperature and circulation play an important role[226]. Areas of cold water and deep-water formation — like the Southern Ocean and North Atlantic — are sinks for $^{14}CO_2$ while the warm water along the equator can release $^{14}CO_2$ into the atmosphere. Carbon can reside in the deep ocean long enough for radioactive decay to occur, resulting in carbon ages exceeding 2,000 years in the deep North Pacific. Carbon moves throughout the ocean and can alter the ^{14}C age of surface water through upwelling and horizontal circulation. This slow exchange of radiocarbon between the ocean and atmosphere results in the surface ocean having an average age of ~400–500 years[83,227,228], an effect known as the MRE.

Ocean surveys of seawater DIC in the 1970s and the 1990s show discreet snapshots of ocean CO_2 uptake and the age of carbon in different ocean basins[229,230]. The differences in radiocarbon age from the ocean surface and depths have provided a history of ocean circulation and ventilation **[G]**[231]. Changes in ventilation are related to Meridional Overturning Circulation, and radiocarbon measurement of planktonic foraminifera coupled with benthic foraminifera have identified key periods of changing ocean circulation during major climatic shifts, like the Glacial to Interglacial climate shifts[141,232-234]. Deep sea corals that have been independently aged using uranium-thorium dating coupled with radiocarbon have shown that deep water in the Southern Ocean was sufficiently old during the last glacial maximum to suggest that a release of this carbon into the atmosphere explains the observed increase of atmospheric CO_2 and the decrease of atmospheric radiocarbon observed from 17,000–12,000 years ago[235].

Atmospheric nuclear weapon tests responsible for the bomb peak also mixed into the oceans, thereby increasing surface ^{14}C. The surface ocean bomb ^{14}C peaked approximately 10 years after the atmosphere[226]. Corals from the Galapagos Islands display clear patterns of ^{14}C variability integrated into their skeletons in proportion to ^{14}C variability of surface seawater. The corals bands were formed with higher ^{14}C during El Nino years and with no to low upwelling and lower ^{14}C during normal circulation years[236].

Organic carbon also makes up a significant part of the oceanic carbon pool and can be divided into two main components: DOC (< 0.8µm in size) and POC (> 0.8µm in size)[237]. Studies using

665 radiocarbon measurements of POC and DOC provide detailed insights into biogeochemical
666 cycling in the ocean[238-242]. POC is produced in the surface ocean and is responsible for
667 transporting carbon to the deep ocean and sediments; it retains the ^{14}C signature of the
668 surface ocean[243-245]. The DOC pool contains nearly the same amount of carbon as the
669 atmosphere but is highly variable, with ^{14}C ages ranging between 2,000 and 6,000 years [238,240].

670 **[H2] Biomedical applications**

671 The endogenous capacity of many cell types to renew, in health and pathology, is unknown.
672 Cell regeneration is most often studied by analysing markers of proliferating cells, providing a
673 good indication of the number of cells in cell cycle at any given time, but provides no
674 information as to the cells that survive and stably integrate into the mature tissue. Other
675 methods that provide information about adult-generated cells rely on radioactive or toxic
676 compounds, or fail to provide information about cell turnover across the lifespan of the
677 individual. Such limitations prompted the investigation of whether ^{14}C integrated into genomic
678 DNA mirror atmospheric levels at the time the cell was formed, and could be used to
679 retrospectively determine the age of a population of cells[246]. Thanks to the ^{14}C bomb peak
680 (BOX 4) the concept is straightforward, but the practice has a few issues to take into
681 consideration (BOX 5).

682 Many studies have used radiocarbon dating of DNA to determine cell age, providing important
683 insights into the maintenance and repair of human tissues and organs (Figure 7).
684 Investigations of neuronal turnover in the adult human brain have shown that for many brain
685 regions, no new neurons are generated after birth[246-249], however other brain regions harbour
686 an innate capacity to make new neurons throughout adulthood or in response to injury[250,251].
687 Non-neuronal cells of the brain, such as the cells forming the insulating myelin around the
688 nerve cells (oligodendrocytes) and the immune cells of the brain (microglia), have also been
689 investigated with radiocarbon dating, contributing significantly to our understanding of the
690 maintenance and renewal of these cells during normal brain aging and injury[252,253]. Cell
691 turnover analyses in the heart, including cardiomyocytes, have revealed low levels of cell
692 turnover during adulthood[254,255]. Such data suggests that it may be realistic to target
693 therapeutics which augment endogenous cell renewal for the treatment of cardiac disease.
694 Radiocarbon dating has also been applied to fat cells, showing that adult humans renew their

fat cells at an average rate of 10% per year [256]. Brain tumour growth dynamics and T-cell homeostasis in humans have also been determined using radiocarbon dating[257,258].

Radiocarbon dating is not restricted to DNA and studying cell turnover. Alternative applications, such as measuring lipid turnover in fat tissue[259-261] and myelin turnover in oligodendrocytes[252] have provided important insights into the factors contributing to obesity and weight loss maintenance as well as neuronal circuitry and plasticity, respectively.

[H2] Cultural Heritage

Protection and conservation studies of tangible cultural heritage frequently use radiocarbon dating, although historic data often provide the chronological context for many items. The first radiocarbon dating studies published in 1949 as a part of curve of knowns **[G]**[3] included acacia wood from the tomb of Pharaoh Zoser (Djoser), as well as a range of archaeological textiles and wood from Egypt and North and South America [3,262,263]. Considering that the technological developments at the time meant that several grams of material were required, the sacrifice was remarkable. With the advance of the AMS technique, radiocarbon dating of antique and art objects has become routine.

Collecting a few milligrams of material is still destructive therefore sampling and radiocarbon dating in cultural heritage studies requires additional care and considerations[72,73]. Depending on the time range of the studied items, the type of material and its state of preservation and possible conservation, the amount of required sample may differ. Nowadays, minute samples (tens of micrograms of carbon) can be dated, at the expense of precision. The characteristic complications of the calibration curve — which plague the last 500 years of the time scale[8] and form the Vinci and Stradivarius age plateaus **[G]** [51] — increase the age range of numerous artworks when their radiocarbon ages are calibrated. Nevertheless, the need for radiocarbon dating of manuscripts, paintings, textiles, statutes, musical instruments and objects of everyday use such as furniture and buildings is growing and treatment methods to optimize both sample size of various materials and precision are being developed[264] (Supplementary Table 2). Removal of exogenous carbon such as varnishes or consolidation material using solvents is crucial for accurate and precise dating and for the detection of forgeries[265-268]. Radiocarbon dating of the construction of buildings and monuments is possible with selection of organic remains preserved in mortar or plaster, and AMS has been used to measure ^{14}C in CO_2 trapped in the binder during the consolidation phase [269-273].

Thorough spectral analysis and characterization methods of sample material is essential in choosing most promising fraction or component. For example, proper selection of the binder or pigments from paintings for radiocarbon dating requires characterization of the paint layer using FTIR[274,275], Raman spectroscopy, X-ray fluorescence[276], X-ray diffraction and/or gas chromatography-mass spectrometry [277-280]. These tools are also useful to control the purity of fibers, wood and paper. For paper, the source material of cellulose must be identified in order to support interpretation of the radiocarbon age[281]. FTIR and polarized light microscopy analysis of textiles helps to screen for the presence of synthetic fibers, which are often derived from sources of ^{14}C-free fossil carbon. For the analysis of mortars and plasters, prior to sample selection and radiocarbon dating, petrographic analysis and characterization of their chemical and mineralogical composition using x-ray fluorescence and x-ray diffraction must take place [270-272]. Similarly, metallurgic analysis of iron objects and estimates of carbon content precede the dating of pre-industrial iron objects[282-284]. Finally, interpretation of results requires a combination of all available information: art history, art analysis or provenance research. Bayesian models, which include prior information such as artist's creative period, might be helpful in narrowing the calibrated calendar ages[280,285].

A unique potential of radiocarbon dating for ancient trees has been demonstrated by dating the oldest African baobabs[286]. Old trees have lifespans of several generations and are part of cultural heritage, thanks to their cultural, spiritual and symbolic values. Protection of ancient trees requires knowledge of their age but also understanding of their growth architecture[287,288]. Sampling living trees requires care and ethical conduct, however ancient trees usually have complicated structures and offer opportunities to sample in hollow and exposed places [289]. Such wood is free of conservation therefore preparation for radiocarbon dating is straightforward, contrary to most anthropogenic objects. More examples of dating of ancient trees can be found in Supplementary Table 2).

[H2] Forensics

[H3] Age determination of human remains

Radiocarbon dating of human remains can be used to estimate the age of a person, and can significantly assist authorities when attempting to solve unidentified homicides as well as facilitate identification in mass disasters. Dependent on the stage of preservation, analysis of bone lipids, hair and skin can provide information on the year of death[290]. Since bone undergoes

remodelling across the lifespan, the age of bone does not always reflect person age, and cannot be used to reliably estimate date of birth — with an exception of the petrous bone, which is formed during the postnatal period[291]. Radiocarbon dating of tooth enamel has been used to estimate the date of birth of an individual[292]. Tooth enamel is not remodelled or exchanged during the lifespan and this analysis revealed that when calibrated for enamel formation time, dental enamel provides a remarkably accurate estimate of a person's year of birth[246]. In one example, where radiocarbon dating (and other forensic methodology) was applied to a cold case, the legal identification of a young boy who had died approximately 40 years earlier was made, resulting in the repatriation of the boy's remains and closure for the family[293].

Radiocarbon dating of bone and tooth together with stable isotope analysis of tooth enamel[294] and dental racemization analysis[295] can provide police and forensic authorities with an estimated year of birth, date of death and information about the geographical origin of an individual [294,296-299]. In addition to dental enamel, radiocarbon dating of the eye lens has identified that the crystalline formation of the lens takes place almost entirely around the time of birth[300] (Figure 7). The precision of radiocarbon dating the eye lens is similar to that of dental enamel analysis, and has led to the suggestion that the technique could be used as a forensic tool for age determination[301].

[H3] Wildlife conservation and protection

Measurements of bomb peak ^{14}C help to estimate the time of death of an individual animal, and therefore has a potential to trace products made illegally from the tissue of protected animals or plants. The Convention on International Trade in Endangered Species of Wild Flora and Fauna (CITES) was adopted in 1973 in order to ensure that trade in wildlife is legal and sustainable; it currently covers over 35,000 species. Radiocarbon dating using the bomb peak provides an excellent tool for the detection of illegal trade of ivory and tissue of other protected animals [302-306]. Combined with stable isotopes, DNA analysis and dendrochronology, radiocarbon dating is used to monitor trade in timber[307,308] or poached cycads[309]. However, the atmospheric bomb peak[197] is fading due to the Suess effect (BOX 3), and the radiocarbon dating of future specimens will require the support of the stable carbon isotopes[310].

[H3] Biofuels

Measurement of ^{14}C also has important applications in discriminating the fossil-derived carbon fraction from the biogenic-derived carbon fraction in carbon-based compounds. This is important in the general effort to promote the use of CO_2-neutral products, reduce greenhouse gases emissions and mitigate climate change. Fossil-derived products are completely ^{14}C-depleted, while biogenic products mirror the current radiocarbon atmospheric signal. Simple isotopic mass balance equations can be used to accurately calculate the proportions of the two different carbon sources. Several studies have addressed the different methodological aspects associated with this approach and have assessed the achievable precision and accuracy levels. Routine analyses are now performed on polymers[311], bio-fuels [312,313], synthetic gases[314] as well as flue gases from industrial sources[315,316]. Radiocarbon dating using both beta- counting[317] and AMS[314] techniques is now included in different international protocols such as those of the International Organization for Standardization (ISO)[318] and the American Society for Testing and Materials (ASTM)[319].

[H3] Forgeries

Radiocarbon dating has the potential to detect anachronism of materials of cultural heritage, which might indicate forgery. The method has been applied to historic forgeries, including numerous relics created in the Medieval period[320], with the most famous being the Shroud of Turin[321]. One of the first forgeries detected using radiocarbon dating was the Piltdown Skull, which had been created to represent an early ancestor to humans predating *Homo heidelbergensis* and aged over 500,000 years old, but was ultimately dated to 500-100 years old[*322,323*].

The variable atmospheric ^{14}C in the period from mid-17th to mid-20th centuries prevents detection of early forgeries of paintings from these time periods if items were produced before the onset of the bomb peak (Figure 8). Sometimes radiocarbon dating is used as additional proof of forgery detected or suggested by art research and paint analysis[324,325]. Occasionally, radiocarbon dating may prove insufficient if forgers re-used old canvases, as was the case for forgeries of famous paintings from the 19th and 20th centuries. The dating of the organic binding media could provide an alternate solution to this problem, by detecting binder produced shortly before the production of a counterfeit [326]. Forgeries of other objects are common, and the bomb peak provides an important dating tool in this regard. Current due

diligence protocols applied by many radiocarbon laboratories[71] require documentation of objects' origin, which may act as an initial filter on the art market.

[H1] Reproducibility and data deposition

Historically, the success of radiocarbon dating relies on reproducibility and inter-comparison of findings. Multiple laboratories around the world began their radiocarbon dating operations soon after the method has been established by Libby[3,4]. In the following decades, conventions were set and standards defined[327]. It is worth noting that the initial laboratories used beta-counting, and that the procedures were later adopted for AMS, as many conventional laboratories became hybrids that used both approaches (for example, Groningen, Glasgow, Rafter, Arizona, Helsinki, and others).

[H2] Reproducibility

Reproducibility of radiocarbon age is controlled both internally, by analysis of secondary standards and known-age samples, and externally by international laboratory intercomparison projects, in which multiple labs measure a single homogenized sample. Scott et al., [328] provide an overview of the projects performed during the past 3 decades, included a range of material with ages spanning the last 55,000 years. Intercomparison for specific materials such as cremated bones[329], unburned bones[330], wood[331] and charcoal[332] demonstrate reproducibility of radiocarbon age as reported in summary publications [69,331]

[H2] Publishing ^{14}C ages

The conventional ^{14}C ages (RA) and their one standard deviation (1σ), written as RA ± 1σ should be published along with calibrated ages, the calibration curve used and the laboratory number prescribed to the sample by the radiocarbon laboratory. The list of lab codes current and past is published at radiocarbon.org. The rules have been outlined previously[16,17,19,] (BOX 1). For archaeological studies, additional guidelines are given[333,334].

The practice of publishing all the radiocarbon ages produced by ^{14}C laboratories was established early[335,336] and has been continued by some laboratories, such as the Oxford laboratory [337]. The data lists provide ^{14}C ages, their uncertainty, information on the context and preparation methods[338-340]. Otherwise data are published through specific research publications or may be accessed on request or via the database websites of individual

Radiocarbon laboratories (ORAU, Gliwice Radiocarbon Laboratory, ^{14}CARHU, Royal Institute for Cultural Heritage, New Zealand Radiocarbon Database).

The interdisciplinary applications of radiocarbon dating have also resulted in a number of thematic databases representing the archaeology of specific regions or time periods[341-343], dates of volcanic eruptions[344] and ages of soils[345], bones[346], or seafloor sediments[347]. There are also databases that include radiocarbon dates as a part of extensive data sets in the compilation of climatic records from around the globe [348] (also see Supplementary Table 3).

Users may also refer to the IntCal calibration database, in which all data submitted to IntCal are publicly available[8].

[H1] Limitations and optimizations

Radiocarbon dating is destructive and requires a certain amount of carbon, so careful consideration should be given before analysis of very rare or high value materials. The precision and accuracy of the final calibrated calendar age is affected by both the sample's size and its state of preservation. Independent of the precision of analysis, the features of the calibration curve during the time period to which the sample is dated may also limit the precision of calibrated ages[349]. The final limit is imposed on the method by the decay constant of ^{14}C. All ages close to the limit (older than 40,000 years) have to be considered with caution, and beyond 55,000 years the method can seldom be applied.

Modern AMS instruments are stable systems with design optimized for ^{14}C analysis, control software allowing unattended and remotely controlled operations, and have sample throughput of the order of several thousand per year. Uncertainty levels of 0.2–0.3 % are routinely achieved for samples younger than 10,000 years corresponding to 1σ of approximately 15–20 years in the radiocarbon timescale. Sensitivities of the AMS systems for ^{14}C separation allow the measurement of $^{14}C/^{12}C$ ratios as low as 10^{-15}–10^{-16}, which corresponds to the machine blank levels of 60,000–70,000 years. Though the achievable uncertainty levels degenerate as sample age increases, being limited by the statistics associated with ^{14}C counting, the main factor limiting resolution appears to be related to the calibration stage. As shown in Figure 5, while monotonic parts of the calibration curve can result in monomodal, Gaussian-like probability distributions of calendar ages whose width is defined by the curve steepness, sections with high fluctuation result in multimodal

distributions and separate time intervals[350]. This is an intrinsic and unavoidable limitation of the method which, in some cases, makes interpretation of ^{14}C dating results ambiguous. The single-year record of the atmospheric ^{14}C included in part of the current calibration curve (IntCal20)[8] facilitates more accurate calibration of high-resolution measurements, though not necessarily more precise depending on the higher resolved shape of the curve. However IntCal20 does improve both precision and accuracy in cases where Bayesian wiggle-matching **[G]** can be employed using absolute or relative dating information available from tree-ring, varve sequences, high-resolution sampling or by dense archeological stratigraphy as a statistical constraint during calibration, or when large and rapid excursions in the ^{14}C calibration curve can be used as temporal anchor points to produce calendar year dates in combination with tree-ring methodologies[176,351]. The other intrinsic limit is related to the analysis of samples with ages older than ~40,000 years and close to the limit of the method. For these samples large uncertainties are already associated with ^{14}C determination as due to the limited number of residual ^{14}C atoms while the relative effect of blank correction becomes larger, further reducing precision and time resolution[352].

Independent of analytical and methodological limitations, radiocarbon dating can fail or provide inconclusive answers due to the limited budget dedicated to the analysis. Close collaboration with radiocarbon research laboratories is a possible solution to this problem.

[H1] Outlook

[H2] Measurement techniques

From the technical and instrumental point of view the main developments will likely be a further downscaling of AMS spectrometer dimensions. This trend started 10–15 years ago, mainly due to the pioneering work at the Laboratory for Ion Beam Physics at ETH Zurich. Since then, many of the criterions from the early days of AMS have been broken. For example, the need for a post-stripping of high positive charge states and then high acceleration voltages (2–3 MV) for effective removal of molecular isobaric interferences, are no longer necessary.

A different route towards machine size reduction is the use of positive ion mass spectrometry. First developed at the Scottish Universities Environmental Research Centre (SUERC), this technique is based on the use of positive carbon ions produced from CO_2 in an electron cycolotron resonance ion source and then accelerated towards a charge-exchange gas cell.

Here positive ions charge-exchange to negative ones, allowing the effective removal of interfering hydrocarbons and nitrogen[48].

Installation investments and infrastructure costs have significantly decreased at the same time as the equipment has become more compact and easy to operate and maintain. These improvements will allow an increasing number of radiocarbon measurements to be performed in various facilities, completely different from the early days. Integrated designs are also being developed to facilitate measurement of different quantities and parameters simultaneously from the same sample. This is already the case for combined elemental analyzer-isotope ratio mass spectrometry-AMS systems (EA-IRMS-AMS), which can measure carbon and nitrogen stable isotopes, concentration and radiocarbon age[353,354].

[H2] Expanding applications

The future of radiocarbon analysis rests in the variety of possible applications, which are facilitated by the technical and methodological developments of last two decades. The dynamic field of CSRA, which relies on microgram-size samples, is expanding from studies of sedimentary records to art and archeology. There is a growing trend to use specific molecules to date and trace the sources of environmental carbon[63,355]. In archeology, analysis of specific biomarkers, for example in pottery[126] or bones[356], indicates increased potential for using CSRA to analyze cultural heritage objects.

As AMS continues to improve and it becomes possible to measure smaller and smaller samples, the applications of radiocarbon dating will continue to grow. While radiocarbon dating of biological samples now offers powerful insights into the regenerative potential of different tissues and organs in the human brain and body, currently many structures are limited by their size and the ability to isolate 5 million or more cells, or only small biopsy samples are available. Similarly, as scientists' efforts to isolate and purify subcellular structures improve, deeper questions about human cell biology can be approached, such as how nuclear pore protein and mitochondrial turnover impact health, aging and disease. The speed and accessibility of radiocarbon dating has enabled new applications, like in species conservation; radiocarbon dating has been used in determining the age of sharks[357,358]. These studies demonstrated that sharks can live considerably longer than expected and raise concerns that specific shark populations may be considerably more sensitive to human-induced mortality

than previously thought. Radiocarbon dating may thus have even broader applications for species conservation.

[H2] Single year tree-ring ^{14}C

Improvements in AMS dating have also made it feasible to construct multi-millennial sequences of annually resolved atmospheric ^{14}C from calendar dated tree-rings from a wide range of growth locations in the Northern and Southern hemispheres. This opens up a wide range of new possibilities for exploration. Such data will be used to fine-tune the structure of future calibration curves for the last 14,000 years — currently much of this period is still based on measurements of blocks of 10 or more tree-rings. As precision and accuracy of radiocarbon dating instrumentation improves, the development of new ways to approach subtle regional ^{14}C fluctuations related to growing season or the latitude of the samples will increase. The geographic coverage of the tree-ring record has some limitations in this regard because certain regions near the equator, for which annual ^{14}C data for calibration would be most important due to shifting of the intertropical convergence zone, do not typically produce tree-ring series suitable for conventional tree-ring dating methods. However new approaches using stable isotope pattern matching[359] or chemical boundary identification may provide new resources going forward.

These multi-millennial sequences will be invaluable in reconstructing the solar histories necessary for prediction and mitigation of future solar storms which threaten our modern technological infrastructure, and for applications in multi-proxy synchronisation such as synchronizing sequences of contemporaneously produced cosmogenic ^{10}Be from ice cores and ^{14}C from calendar dated tree-ring sequences[360]. These have also been used to reconstruct solar cycles[361] and to examine this in combination with other tree-ring signals to understand the impacts of past solar activity on climate[362]. This work seems set to expand and diversify considerably over the coming years**.**

References

1 Ruben, S. & Kamen, M. D. Radioactive carbon of long half-life. *Physical Review* **57**, 549 (1940).

2 Anderson, E. C. *et al.* Natural Radiocarbon from Cosmic Radiation. *Physical Review* **72**, 931-936 (1947).

3 Arnold, J. R. & Libby, W. F. Age Determinations by Radiocarbon Content - Checks with Samples of Known Age. *Science* **110**, 678-680 (1949).

4 Libby, W. F., Anderson, E. C. & Arnold, J. R. Age Determination by Radiocarbon Content - World-Wide Assay of Natural Radiocarbon. *Science* **109**, 227-228 (1949).

5 Rom, W. *et al.* A detailed 2-year record of atmospheric (CO)-C-14 in the temperate northern hemisphere. *Nuclear Instruments & Methods in Physics Research Section B-Beam Interactions with Materials and Atoms* **161**, 780-785 (2000).

6 Kutschera, W. Applications of accelerator mass spectrometry. *Int J Mass Spectrom* **349**, 203-218 (2013).

7 Kutschera, W. The Half-Life of 14C—Why Is It So Long? *Radiocarbon* **61**, 1135-1142 (2019).

8 Reimer, P. J. *et al.* The IntCal20 Northern Hemisphere Radiocarbon Age Calibration Curve (0–55 cal kBP). *Radiocarbon* **62**, 725-757, doi:10.1017/RDC.2020.41 (2020).

9 Hogg, A. G. *et al.* SHCal20 Southern Hemisphere Calibration, 0–55,000 Years cal BP. *Radiocarbon* **62**, 759-778, doi:10.1017/RDC.2020.59 (2020).

10 Heaton, T. J. *et al.* Marine20—the marine radiocarbon age calibration curve (0–55,000 cal BP). *Radiocarbon* **62**, 779-820 (2020).

11 Santos, G., Southon, J., Griffin, S., Beaupre, S. & Druffel, E. Ultra small-mass AMS 14C sample preparation and analyses at KCCAMS/UCI Facility. *Nuclear Instruments and Methods in Physics Research Section B: Beam Interactions with Materials and Atoms* **259**, 293-302 (2007).

12 Ruff, M. *et al.* A gas ion source for radiocarbon measurements at 200 kV. *Radiocarbon* **49**, 307-314 (2007).

13 Smith, A., Hua, Q., Williams, A., Levchenko, V. & Yang, B. Developments in micro-sample C-14 AMS at the ANTARES AMS facility. *Nuclear Instruments & Methods in Physics Research Section B-Beam Interactions With Materials and Atoms* **268**, 919-923, doi:10.1016/j.nimb.2009.10.064 (2010).

14 Steier, P., Liebl, J., Kutschera, W., Wild, E. M. & Golser, R. Preparation Methods of µg Carbon Samples for ^{14}C Measurements. *Radiocarbon* **59**, 803 (2017).

15 Eglinton, T. I., Aluwihare, L. I., Bauer, J. E., Druffel, E. R. & McNichol, A. P. Gas chromatographic isolation of individual compounds from complex matrices for radiocarbon dating. *Analytical Chemistry* **68**, 904-912 (1996).

16 Reimer, P. J., Brown, T. A. & Reimer, R. W. Discussion: Reporting and calibration of post-bomb C-14 data. *Radiocarbon* **46**, 1299-1304 (2004).

17 Stuiver, M. & Polach, H. A. Reporting of C-14 Data - Discussion. *Radiocarbon* **19**, 355-363 (1977).

18 Mook, W. G. & van der Plicht, J. Reporting C-14 activities and concentrations. *Radiocarbon* **41**, 227-239 (1999).

19 van der Plicht, J. & Hogg, A. A note on reporting radiocarbon. *Quaternary Geochronology* **1**, 237-240 (2006).

20 Stenström, K. E., Skog, G., Georgiadou, E., Genberg, J. & Johansson, A. A guide to radiocarbon units and calculations. *Lund University, Department of Physics internal report*, 1-17 (2011).

21 Paterne, M., Michel, É., Hatté, C. & Dutay, J.-C. in *Paleoclimatology* (eds G. Ramstein *et al.*) 51-71 (Springer International Publishing, 2020).

22 Libby, W. F. Radiocarbon dating. *Chem Brit* **5**, 548-552 (1955).

23 Kromer, B. & Muennich, K. O. in *Radiocarbon after four decades. An interdisciplinary perspective* (eds R.E. Taylor, A. Long, & R.S. Kra) 184-197 (Springer Verlag, 1992).

24 Polach, H. A. in *Radiocarbon After Four Decades* 198-213 (Springer, 1992).

25 Povinec, P. P., Litherland, A. & von Reden, K. F. Developments in radiocarbon technologies: from the Libby counter to compound-specific AMS analyses. *Radiocarbon* **51**, 45-78 (2009).

26 Tudyka, K. *et al.* A low level liquid scintillation spectrometer with five counting modules for 14C, 222Rn and delayed coincidence measurements. *Radiation Measurements* **105**, 1-6 (2017).

27 Theodórsson, P. *et al.* Ultra-stable single-phototube liquid scintillation system for radiocarbon dating. *LSC*, 253-260 (2008).

28 Quiles, A., Kamal, N. S., Abd'el Fatah, M. & Mounir, N. The Ifao Radiocarbon laboratory: A status report. *Radiocarbon* **59**, 1157 (2017).

29 Gudelis, A., Gaigalaitė, L. & Gvozdaitė, R. Application of the absolute method for determination of tritium and radiocarbon in groundwater from radioactive waste facility. *Journal of Radioanalytical and Nuclear Chemistry* **322**, 1391-1396 (2019).

30 Feng, B. *et al.* Application of synthetic benzoic acid technology in environmental radiocarbon monitoring. *Journal of environmental radioactivity* **216**, 106188 (2020).

31 Cuchet, A. *et al.* Authentication of the naturalness of wintergreen (Gaultheria genus) essential oils by gas chromatography, isotope ratio mass spectrometry and radiocarbon assessment. *Industrial Crops and Products* **142**, 111873 (2019).

32 Purser, K. H. *et al.* An attempt to detect stable N-ions from a sputter ion source and some implications of the results for the design of tandems for ultra-sensitive carbon analysis. *Revue de Physique appliquee* **12**, 1487-1492 (1977).

33 Nelson, D. E., Korteling, R. G. & Stott, W. R. Carbon-14: direct detection at natural concentrations. *Science* **198**, 507-508 (1977).

34 Bennett, C. L. *et al.* Radiocarbon dating using electrostatic accelerators: negative ions provide the key. *Science* **198**, 508-510 (1977).

35 Litherland, A., Zhao, X. L. & Kieser, W. Mass spectrometry with accelerators. *Mass spectrometry reviews* **30**, 1037-1072 (2011).

36 Synal, H.-A., Jacob, S. & Suter, M. The PSI/ETH small radiocarbon dating system. *Nuclear Instruments and Methods in Physics Research Section B: Beam Interactions with Materials and Atoms* **172**, 1-7 (2000).

37 Synal, H.-A., Dobeli, M., Jacob, S., Stocker, M. & Suter, M. Radiocarbon AMS towards its low-energy limits. *Nuclear Instruments and Methods in Physics Research Section B: Beam Interactions with Materials and Atoms* **223-224**, 339-345 (2004).

38 Synal, H. A., Schulze-Konig, T., Seiler, M., Suter, M. & Wacker, L. Mass spectrometric detection of radiocarbon for dating applications. *Nuclear Instruments & Methods in Physics Research Section B-Beam Interactions with Materials and Atoms* **294**, 349-352, doi:10.1016/j.nimb.2012.01.026 (2013).

39 Salehpour, M., Håkansson, K., Possnert, G., Wacker, L. & Synal, H.-A. Performance report for the low energy compact radiocarbon accelerator mass spectrometer at Uppsala University. *Nuclear Instruments and Methods in Physics Research Section B: Beam Interactions with Materials and Atoms* **371**, 360-364 (2016).

40 Seiler, M., Maxeiner, S., Wacker, L. & Synal, H.-A. Status of mass spectrometric radiocarbon detection at ETHZ. *Nuclear Instruments and Methods in Physics Research Section B: Beam Interactions with Materials and Atoms* **361**, 245-249 (2015).

41 Fahrni, S., Wacker, L., Synal, H.-A. & Szidat, S. Improving a gas ion source for 14C AMS. *Nuclear Instruments and Methods in Physics Research Section B: Beam Interactions with Materials and Atoms* **294**, 320-327 (2013).

42 Wacker, L. *et al.* A versatile gas interface for routine radiocarbon analysis with a gas ion source. *Nuclear Instruments & Methods in Physics Research Section B-Beam Interactions with Materials and Atoms* **294**, 315-319, doi:10.1016/j.nimb.2012.02.009 (2013).

43 Wacker, L., Lippold, J., Molnar, M. & Schulz, H. Towards radiocarbon dating of single foraminifera with a gas ion source. *Nuclear Instruments & Methods in Physics Research Section B-Beam Interactions With Materials and Atoms* **294**, 307-310, doi:10.1016/j.nimb.2012.08.038 (2013).

44 Haghipour, N. *et al.* Compound-Specific Radiocarbon Analysis by Elemental Analyzer-Accelerator Mass Spectrometry: Precision and Limitations. *Analytical Chemistry* **91**, 2042-2049, doi:10.1021/acs.analchem.8b04491 (2019).

45 Leonard, A., Castle, S., Burr, G. S., Lange, T. & Thomas, J. A wet oxidation method for AMS radiocarbon analysis of dissolved organic carbon in water. *Radiocarbon* **55**, 545-552 (2013).

46 Molnar, M. *et al.* C-14 analysis of groundwater down to the millilitre level. *Nuclear Instruments & Methods in Physics Research Section B-Beam Interactions with Materials and Atoms* **294**, 573-576, doi:10.1016/j.nimb.2012.03.038 (2013).
47 Welte, C. *et al.* Laser Ablation - Accelerator Mass Spectrometry: An Approach for Rapid Radiocarbon Analyses of Carbonate Archives at High Spatial Resolution. *Analytical Chemistry* **88**, 8570-8576, doi:10.1021/acs.analchem.6b01659 (2016).
48 Freeman, S. P., Shanks, R. P., Donzel, X. & Gaubert, G. Radiocarbon positive-ion mass spectrometry. *Nuclear Instruments and Methods in Physics Research Section B: Beam Interactions with Materials and Atoms* **361**, 229-232 (2015).
49 Bayliss, A. Rolling out revolution: using radiocarbon dating in archaeology. *Radiocarbon* **51**, 123-147 (2009).
50 van der Plicht, J., Scott, E., Alekseev, A. & Zaitseva, G. Radiocarbon, the calibration curve and Scythian chronology. *Impact of the Environment on Human Migration in Eurasia* **42**, 45-61 (2004).
51 Jull, A. Accelerator radiocarbon dating of art, textiles, and artifacts. *Nuclear News* **41**, 30-38 (1998).
52 Aitken, M. J. Archaeological dating using physical phenomena. *Rep Prog Phys* **62**, 1333-1376 (1999).
53 Boaretto, E. Radiocarbon and the Archaeological Record: An Integrative Approach for Building an Absolute Chronology for the Late Bronze and Iron Ages of Israel. *Radiocarbon* **57**, 207-216, doi:10.2458/azu_rc.57.18554 (2015).
54 Brock, F., Higham, T. & Ramsey, C. B. Pre-screening techniques for identification of samples suitable for radiocarbon dating of poorly preserved bones. *Journal of archaeological science* **37**, 855-865 (2010).
55 D'Elia, M. *et al.* Evaluation of possible contamination sources in the 14C analysis of bone samples by FTIR spectroscopy. *Radiocarbon* **49**, 201-210 (2007).
56 Brock, F. *et al.* Testing the Effectiveness of Protocols for Removal of Common Conservation Treatments for Radiocarbon Dating. *Radiocarbon* **60**, 35-50, doi:10.1017/RDC.2017.68 (2018).
57 Devièse, T. *et al.* A multi-analytical approach using FTIR, GC/MS and Py-GC/MS revealed early evidence of embalming practices in Roman catacombs. *Microchem J* **133**, 49-59 (2017).
58 Yizhaq, M. *et al.* Quality controlled radiocarbon dating of bones and charcoal from the early Pre-Pottery Neolithic B (PPNB) of Motza (Israel). *Radiocarbon* **47**, 193-206 (2005).
59 Sponheimer, M. *et al.* Saving Old Bones: a non-destructive method for bone collagen prescreening. *Scientific reports* **9**, 1-7 (2019).
60 Naito, Y. I., Yamane, M. & Kitagawa, H. A protocol for using attenuated total reflection Fourier-transform infrared spectroscopy for pre-screening ancient bone collagen prior to radiocarbon dating. *Rapid Communications in Mass Spectrometry* **34**, e8720 (2020).
61 Brock, F., Higham, T., Ditchfield, P. & Ramsey, C. B. Current Pretreatment Methods for Ams Radiocarbon Dating at the Oxford Radiocarbon Accelerator Unit (Orau). *Radiocarbon* **52**, 103-112, doi:Doi 10.1017/S0033822200045069 (2010).
62 Hajdas, I. The Radiocarbon dating method and its applications in Quaternary studies. *Quaternary Science Journal - Eiszeitalter und Gegenwart* **57**, 2-24 (2008).
63 Ingalls, A. E. & Pearson, A. Compound-Specific Radiocarbon Analysis. *Oceanography* **18**, 18-31 (2005).
64 Ingalls, A. E. *et al.* HPLC purification of higher plant-dervied lignin phenols for compound specific radiocarbon analysis. *Analytical chemistry* **82**, 8931-8938 (2010).
65 Ishikawa, N. F. *et al.* Improved Method for Isolation and Purification of Underivatized Amino Acids for Radiocarbon Analysis. *Analytical Chemistry* **90**, 12035-12041, doi:10.1021/acs.analchem.8b02693 (2018).
66 Blattmann, T. M., Montluçon, D. B., Haghipour, N., Ishikawa, N. F. & Eglinton, T. I. Liquid Chromatographic Isolation of Individual Amino Acids Extracted From Sediments for Radiocarbon Analysis. *Front Mar Sci* **7**, 174 (2020).

67 Mann, W. B. An International Reference Material for Radiocarbon Dating. *Radiocarbon* **25**, 519-527 (1983).
68 Rozanski, K. *et al.* The IAEA 14 C intercomparison exercise 1990. *Radiocarbon* **34**, 506-519 (1992).
69 Scott, E. M., Naysmith, P. & Cook, G. T. Why do we need 14C inter-comparisons?: The Glasgow-14C inter-comparison series, a reflection over 30 years. *Quaternary Geochronology* **43**, 72-82 (2018).
70 Huysecom, E., Hajdas, I., Renold, M.-A., Synal, H.-A. & Mayor, A. The "Enhancement" of Cultural Heritage by AMS Dating: Ethical Questions and Practical Proposals. *Radiocarbon* **59**, 559-563 (2017).
71 Hajdas, I. *et al.* Radiocarbon Dating and the Protection of Cultural Heritage. *Radiocarbon* **61**, 1133-1134, doi:10.1017/Rdc.2019.100 (2019).
72 Freedman, J., van Dorp, L. & Brace, S. Destructive sampling natural science collections: an overview for museum professionals and researchers. *Journal of Natural Science Collections* **5**, 21-34 (2018).
73 (AIC), A. I. f. C. o. H. A. W. *Code of Ethics and Guidelines for Practice*.
74 Séguin, F. H., Schneider, R. J., Jones, G. A. & Karl, F. Optimized data analysis for AMS radiocarbon dating. *Nuclear Instruments and Methods in Physics Research Section B: Beam Interactions with Materials and Atoms* **92**, 176-181 (1994).
75 Rom, W. *et al.* Systematic investigations of 14C measurements at the Vienna Environmental Research Accelerator. *Radiocarbon* **40**, 255-263 (1997).
76 McNichol, A. P., Jull, A. J. T. & Burr, G. S. Converting AMS data to radiocarbon values: Considerations and conventions. *Radiocarbon* **43**, 313-320 (2001).
77 Wacker, L., Christl, M. & Synal, H. A. Bats: A new tool for AMS data reduction. *Nuclear Instruments & Methods in Physics Research Section B-Beam Interactions with Materials and Atoms* **268**, 976-979 (2010).
78 Craig, H. Carbon-13 in Plants and the Relationships between Carbon-13 and Carbon-14 Variations in Nature. *Journal of Geology* **62**, 115-149 (1954).
79 Welte, C. *et al.* Towards the limits: Analysis of microscale 14C samples using EA-AMS. *Nuclear Instruments and Methods in Physics Research Section B: Beam Interactions with Materials and Atoms* **437**, 66-74 (2018).
80 Santos, G. M. *et al.* AMS C-14 sample preparation at the KCCAMS/UCI facility: Status report and performance of small samples. *Radiocarbon* **49**, 255-269 (2007).
81 Sookdeo, A. *et al.* Quality dating: a well-defined protocol implemented at ETH for high-precision 14C-dates tested on late glacial wood. *Radiocarbon* **62**, 891-899 (2020).
82 Alves, E. Q., Macario, K., Ascough, P. & Bronk Ramsey, C. The Worldwide Marine Radiocarbon Reservoir Effect: Definitions, Mechanisms, and Prospects. *Reviews of Geophysics* **56**, 278-305, doi:10.1002/2017rg000588 (2018).
83 Stuiver, M., Pearson, G. W. & Braziunas, T. Radiocarbon Age Calibration of Marine Samples Back to 9000 Cal Yr Bp. *Radiocarbon* **28**, 980-1021 (1986).
84 Ascough, P., Cook, G. & Dugmore, A. Methodological approaches to determining the marine radiocarbon reservoir effect. *Progress in Physical Geography* **29**, 532-547 (2005).
85 Reimer, P. J. & Reimer, R. W. A marine reservoir correction database and on-line interface. *Radiocarbon* **43**, 461-463 (2001).
86 Philippsen, B. The freshwater reservoir effect in radiocarbon dating. *Heritage Science* **1**, 1-19 (2013).
87 Keaveney, E. M. & Reimer, P. J. Understanding the variability in freshwater radiocarbon reservoir offsets: a cautionary tale. *Journal of Archaeological Science* **39**, 1306-1316 (2012).
88 Cook, G. T. *et al.* Best practice methodology for 14C calibration of marine and mixed terrestrial/marine samples. *Quaternary Geochronology* **27**, 164-171 (2015).
89 Arneborg, J. *et al.* Change of diet of the Greenland Vikings determined from stable carbon isotope analysis and 14C dating of their bones. *Radiocarbon* **41**, 157-168 (1999).

90 MacAvoy, S. E., Macko, S. A. & Garman, G. C. Tracing Marine Biomass into Tidal Freshwater Ecosystems Using Stable Sulfur Isotopes. *The Science of Nature* **85**, 544-546, doi:10.1007/s001140050546 (1998).
91 Beesley, L. S. *et al.* new insights into the food web of an Australian tropical river to inform water resource management. *Scientific reports* **10**, 1-12 (2020).
92 Ascough, P. L. *et al.* Radiocarbon reservoir effects in human bone collagen from northern Iceland. *Journal of Archaeological Science* **39**, 2261-2271 (2012).
93 Fernandes, R., Millard, A. R., Brabec, M., Nadeau, M.-J. & Grootes, P. Food reconstruction using isotopic transferred signals (FRUITS): a Bayesian model for diet reconstruction. *PloS one* **9**, e87436 (2014).
94 Cheng, H. *et al.* Atmospheric 14C/12C changes during the last glacial period from Hulu Cave. *Science* **362**, 1293-1297 (2018).
95 Reimer, P. J. *et al.* Selection and Treatment of Data for Radiocarbon Calibration: An Update to the International Calibration (Intcal) Criteria. *Radiocarbon* **55**, 1923-1945 (2013).
96 Lechleitner, F. A. *et al.* Hydrological and climatological controls on radiocarbon concentrations in a tropical stalagmite. *Geochimica et Cosmochimica Acta* **194**, 233-252 (2016).
97 Yeman, C. *et al.* Unravelling Quasi-Continuous 14 C Profiles by Laser Ablation AMS. *Radiocarbon* **62**, 453-465 (2020).
98 Ramsey, C. OxCal 4. 4. Electronic document. (2021).
99 Stuiver, M., Reimer, P. J. & Reimer, R. W. CALIB 8.2 [www program]. (2021).
100 Santos, G. M., Granato-Souza, D., Barbosa, A. C., Oelkers, R. & Andreu-Hayles, L. Radiocarbon analysis confirms annual periodicity in Cedrela odorata tree rings from the equatorial Amazon. *Quaternary Geochronology* **58**, 101079, doi:https://doi.org/10.1016/j.quageo.2020.101079 (2020).
101 Hua, Q., Barbetti, M. & Rakowski, A. Z. Atmospheric Radiocarbon for the Period 1950-2010. *Radiocarbon* **55**, 2059-2072, doi:DOI 10.2458/azu_js_rc.v55i2.16177 (2013).
102 Buck, C. E., Kenworthy, J. B., Litton, C. D. & Smith, A. F. Combining archaeological and radiocarbon information: a Bayesian approach to calibration. *Antiquity* **65**, 808 (1991).
103 Ramsey, C. B. Bayesian Analysis of Radiocarbon Dates. *Radiocarbon* **51**, 337-360 (2009).
104 van de Schoot, R. *et al.* Bayesian statistics and modelling. *Nature Reviews Methods Primers* **1**, 1, doi:10.1038/s43586-020-00001-2 (2021).
105 Hajdas, I. & Michczynski, A. Age-Depth Model of Lake Soppensee (Switzerland) Based on the High-Resolution C-14 Chronology Compared with Varve Chronology. *Radiocarbon* **52**, 1027-1040 (2010).
106 Buck, C. E. & Meson, B. On being a good Bayesian. *World Archaeol* **47**, 567-584 (2015).
107 Ramsey, C. B. Radiocarbon calibration and analysis of stratigraphy: The OxCal program. *Radiocarbon* **37**, 425-430 (1995).
108 Buck, C. E., Christen, J. A. & James, G. N. BCal: an on-line Bayesian radiocarbon calibration tool. *Internet archaeology* **7**, 1192-1201 (1999).
109 Lougheed, B. & Obrochta, S. MatCal: Open source Bayesian 14 C age calibration in MatLab. *Journal of Open Research Software* **4** (2016).
110 Lanos, P. & Dufresne, P. (2019).
111 Renfrew, C. Before Civilization. The Radiocarbon Revolution and Prehistoric Europe. London. (1973).
112 Ramsey, C. B., Schulting, R., Bazaliiskii, V., Goriunova, O. & Weber, A. Spatio-temporal patterns of cemetery use among Middle Holocene hunter-gatherers of Cis-Baikal, Eastern Siberia. *Archaeol Res Asia* **25**, 100253 (2021).
113 Wood, R. From revolution to convention: the past, present and future of radiocarbon dating. *Journal of Archaeological Science* **56**, 61-72 (2015).
114 Wood, R. *et al.* Testing the ABOx-SC method: Dating known-age charcoals associated with the Campanian Ignimbrite. *Quaternary Geochronology* **9**, 16-26, doi:10.1016/j.quageo.2012.02.003 (2012).

115 Jacobi, R. M., Higham, T. F. G. & Ramsey, C. B. AMS radiocarbon dating of Middle and Upper Palaeolithic bone in the British Isles: improved reliability using ultrafiltration. *Journal of Quaternary Science* **21**, 557-573 (2006).
116 Cersoy, S. *et al.* Radiocarbon dating minute amounts of bone (3–60 mg) with ECHoMICADAS. **7**, 1-8 (2017).
117 Fewlass, H. *et al.* Size matters: radiocarbon dates of< 200 µg ancient collagen samples with AixMICADAS and its gas ion source. *Radiocarbon* **60**, 425-439 (2017).
118 Fewlass, H. *et al.* Pretreatment and gaseous radiocarbon dating of 40–100 mg archaeological bone. **9**, 1-11 (2019).
119 Douka, K., Hedges, R. E. & Higham, T. F. Improved AMS 14 C dating of shell carbonates using high-precision X-ray diffraction and a novel density separation protocol (CarDS). *Radiocarbon* **52**, 735-751 (2010).
120 Marom, A., McCullagh, J. S., Higham, T. F., Sinitsyn, A. A. & Hedges, R. E. Single amino acid radiocarbon dating of Upper Paleolithic modern humans. *Proceedings of the National Academy of Sciences* **109**, 6878-6881 (2012).
121 Deviese, T. *et al.* Increasing accuracy for the radiocarbon dating of sites occupied by the first Americans. *Quaternary Science Reviews* **198**, 171-180 (2018).
122 Higham, T. *et al.* The timing and spatiotemporal patterning of Neanderthal disappearance. *Nature* **512**, 306-309 (2014).
123 Fewlass, H. *et al.* A 14C chronology for the Middle to Upper Palaeolithic transition at Bacho Kiro Cave, Bulgaria. *Nature Ecology & Evolution* **4**, 794-801, doi:10.1038/s41559-020-1136-3 (2020).
124 Spindler, L. *et al.* Dating the last Middle Palaeolithic of the Crimean Peninsula: New hydroxyproline AMS dates from the site of Kabazi II. *Journal of Human Evolution* **156**, 102996, doi:https://doi.org/10.1016/j.jhevol.2021.102996 (2021).
125 Berstan, R. *et al.* Direct dating of pottery from its organic residues: new precision using compound-specific carbon isotopes. *Antiquity* **82**, 702-713 (2008).
126 Casanova, E. *et al.* Accurate compound-specific 14C dating of archaeological pottery vessels. *Nature*, doi:10.1038/s41586-020-2178-z (2020).
127 Zuo, X. *et al.* Dating rice remains through phytolith carbon-14 study reveals domestication at the beginning of the Holocene. *Proceedings of the National Academy of Sciences* **114**, 6486-6491 (2017).
128 Boaretto, E. Dating Materials in Good Archaeological Contexts: The Next Challenge for Radiocarbon Analysis. *Radiocarbon* **51**, 275-281, doi:Doi 10.1017/S0033822200033804 (2009).
129 Santos, G. M. *et al.* The phytolith 14 C puzzle: a tale of background determinations and accuracy tests. *Radiocarbon* **52**, 113-128 (2010).
130 Santos, G. M., Masion, A. & Alexandre, A. When the carbon being dated is not what you think it is: Insights from phytolith carbon research. *Quaternary Science Reviews* **197**, 162-174 (2018).
131 Charlton, S. *et al.* Finding Britain's last hunter-gatherers: A new biomolecular approach to 'unidentifiable'bone fragments utilising bone collagen. *Journal of Archaeological Science* **73**, 55-61 (2016).
132 Devièse, T. *et al.* Compound-specific radiocarbon dating and mitochondrial DNA analysis of the Pleistocene hominin from Salkhit Mongolia. *Nature communications* **10**, 1-7 (2019).
133 Zeidler, J. A., Buck, C. E. & Litton, C. D. Integration of archaeological phase information and radiocarbon results from the Jama River Valley, Ecuador: a Bayesian approach. *Latin American Antiquity*, 160-179 (1998).
134 Crema, E. R. & Kobayashi, K. i. A multi-proxy inference of Jōmon population dynamics using bayesian phase models, residential data, and summed probability distribution of 14C dates. *Journal of Archaeological Science* **117**, 105136 (2020).
135 Gakuhari, T. *et al.* Radiocarbon dating of one human and two dog burials from the Kamikuroiwa rock shelter site, Ehime Prefecture. *Anthropol Sci*, 150309 (2015).
136 Bayliss, A. *et al.* Getting to the bottom of it all: a Bayesian approach to dating the start of Çatalhöyük. *Journal of World Prehistory* **28**, 1-26 (2015).

137 Regev, J. *et al.* Radiocarbon dating and microarchaeology untangle the history of Jerusalem's Temple Mount: A view from Wilson's Arch. *Plos one* **15**, e0233307 (2020).
138 Piotrowska, N., Blaauw, M., Mauquoy, D. & Chambers, F. M. Constructing deposition chronologies for peat deposits using radiocarbon dating. *Mires and Peat* **7**, 1-14 (2011).
139 Francisquini, M. I. *et al.* Cold and humid Atlantic Rainforest during the last glacial maximum, northern Espírito Santo state, southeastern Brazil. *Quaternary Science Reviews* **244**, 106489, doi:https://doi.org/10.1016/j.quascirev.2020.106489 (2020).
140 Staff, R. *et al.* The multiple chronological techniques applied to the Lake Suigetsu SG06 sediment core, central Japan. *Boreas* **42**, 259-266, doi:10.1111/j.1502-3885.2012.00278.x (2013).
141 Broecker, W. *et al.* Ventilation of the glacial deep Pacific Ocean. *Science* **306**, 1169-1172, doi:DOI 10.1126/science.1102293 (2004).
142 Sikes, E. L., Samson, C. R., Guilderson, T. P. & Howard, W. R. Old radiocarbon ages in the southwest Pacific Ocean during the last glacial period and deglaciation. *Nature . Jun* **405**, 555-559 (2000).
143 Joerin, U., Nicolussi, K., Fischer, A., Stocker, T. & Schluchter, C. Holocene optimum events inferred from subglacial sediments at Tschierva Glacier, Eastern Swiss Alps. *Quaternary Science Reviews* **27**, 337-350, doi:10.1016/j.quascirev.2007.10.016 (2008).
144 Bolton, A., Goodkin, N. F., Druffel, E. R. M., Griffin, S. & Murty, S. A. Upwelling of Pacific Intermediate Water in the South China Sea Revealed by Coral Radiocarbon Record. *Radiocarbon* **58**, 37-53, doi:10.1017/RDC.2015.4 (2016).
145 Hirabayashi, S. *et al.* Insight into Western Pacific Circulation from South China Sea Coral Skeletal Radiocarbon. *Radiocarbon* **61**, 1923-1937, doi:10.1017/RDC.2019.145 (2019).
146 Hua, Q. *et al.* Robust chronological reconstruction for young speleothems using radiocarbon. *Quaternary Geochronology* **14**, 67-80 (2012).
147 Akers, P. D. *et al.* Integrating U-Th, 14C, and 210Pb methods to produce a chronologically reliable isotope record for the Belize River Valley Maya from a low-uranium stalagmite. *The Holocene* **29**, 1234-1248 (2019).
148 Therre, S. *et al.* Climate-induced speleothem radiocarbon variability on Socotra Island from the Last Glacial Maximum to the Younger Dryas. *Climate of the Past* **16**, 409-421 (2020).
149 Moska, P., Jary, Z., Adamiec, G. & Bluszcz, A. Chronostratigraphy of a loess-palaeosol sequence in Biały Kościół, Poland using OSL and radiocarbon dating. *Quaternary International* **502**, 4-17 (2019).
150 Pigati, J. S., McGeehin, J. P., Muhs, D. R., Grimley, D. A. & Nekola, J. C. Radiocarbon dating loess deposits in the Mississippi Valley using terrestrial gastropod shells (Polygyridae, Helicinidae, and Discidae). *Aeolian Research* **16**, 25-33 (2015).
151 Moine, O. *et al.* The impact of Last Glacial climate variability in west-European loess revealed by radiocarbon dating of fossil earthworm granules. *Proceedings of the National Academy of Sciences* **114**, 6209-6214 (2017).
152 Bond, G. *et al.* Correlations between Climate Records from North-Atlantic Sediments and Greenland Ice. *Nature* **365**, 143-147, doi:DOI 10.1038/365143a0 (1993).
153 Grimm, E. C. *et al.* Evidence for warm wet Heinrich events in Florida. *Quaternary Science Reviews* **25**, 2197-2211 (2006).
154 Prokopenko, A. A., Williams, D. F., Karabanov, E. B. & Khursevich, G. K. Continental response to Heinrich events and Bond cycles in sedimentary record of Lake Baikal, Siberia. *Global and Planetary Change* **28**, 217-226 (2001).
155 Obrochta, S. *et al.* Mt. Fuji Holocene eruption history reconstructed from proximal lake sediments and high-density radiocarbon dating. *Quaternary Science Reviews* **200**, 395-405 (2018).
156 Vandergoes, M. *et al.* A revised age for the Kawakawa/Oruanui tephra, a key marker for the Last Glacial Maximum in New Zealand. *Quaternary Science Reviews* **74**, 195-201, doi:10.1016/j.quascirev.2012.11.006 (2013).

157 Sevink, J., Bakels, C., Van Hall, R. & Dee, M. Radiocarbon dating distal tephra from the Early Bronze Age Avellino eruption (EU-5) in the coastal basins of southern Lazio (Italy): Uncertainties, results, and implications for dating distal tephra. *Quaternary Geochronology* **63**, 101154 (2021).
158 Danišík, M. *et al.* Sub-millennial eruptive recurrence in the silicic Mangaone Subgroup tephra sequence, New Zealand, from Bayesian modelling of zircon double-dating and radiocarbon ages. *Quaternary Science Reviews* **246**, 106517 (2020).
159 Nicolussi, K., Spötl, C., Thurner, A. & Reimer, P. J. Precise radiocarbon dating of the giant Köfels landslide (Eastern Alps, Austria). *Geomorphology* **243**, 87-91 (2015).
160 Bertolini, G., Casagli, N., Ermini, L. & Malaguti, C. Radiocarbon data on Lateglacial and Holocene landslides in the Northern Apennines. *Natural Hazards* **31**, 645-662 (2004).
161 Borgatti, L. & Soldati, M. Landslides as a geomorphological proxy for climate change: a record from the Dolomites (northern Italy). *Geomorphology* **120**, 56-64 (2010).
162 Talling, P. J. Fidelity of turbidites as earthquake records. *Nature Geoscience*, 1-3 (2021).
163 Shirahama, Y. *et al.* Detailed paleoseismic history of the Hinagu fault zone revealed by the high-density radiocarbon dating and trenching survey across a surface rupture of the 2016 Kumamoto earthquake, Kyushu, Japan. *Island Arc* **30**, e12376 (2021).
164 Ishizawa, T. *et al.* Sequential radiocarbon measurement of bulk peat for high-precision dating of tsunami deposits. *Quaternary Geochronology* **41**, 202-210 (2017).
165 Bondevik, S., Stormo, S. K. & Skjerdal, G. Green mosses date the Storegga tsunami to the chilliest decades of the 8.2 ka cold event. *Quaternary Science Reviews* **45**, 1-6 (2012).
166 Williams, M. *et al.* Late Quaternary floods and droughts in the Nile valley, Sudan: new evidence from optically stimulated luminescence and AMS radiocarbon dating. *Quaternary Science Reviews* **29**, 1116-1137, doi:10.1016/j.quascirev.2010.02.018 (2010).
167 Shen, H., Yu, L., Zhang, H., Zhao, M. & Lai, Z. OSL and radiocarbon dating of flood deposits and its paleoclimatic and archaeological implications in the Yihe River Basin, East China. *Quaternary Geochronology* **30**, 398-404 (2015).
168 Williams, M. *et al.* Late Quaternary floods and droughts in the Nile valley, Sudan: new evidence from optically stimulated luminescence and AMS radiocarbon dating. *Quaternary Science Reviews* **29**, 1116-1137 (2010).
169 Miyake, F., Nagaya, K., Masuda, K. & Nakamura, T. A signature of cosmic-ray increase in AD 774–775 from tree rings in Japan. *Nature* **486**, 240-242 (2012).
170 Miyake, F. *et al.* Search for Annual C-14 Excursions in the Past. *Radiocarbon* **59**, 315-320 (2017).
171 Miyake, F., Masuda, K. & Nakamura, T. Another rapid event in the carbon-14 content of tree rings. *Nature communications* **4**, 1-6 (2013).
172 Miyake, F. *et al.* Large C-14 excursion in 5480 BC indicates an abnormal sun in the mid-Holocene. *Proceedings of the National Academy of Sciences of the United States of America* **114**, 881-884, doi:10.1073/pnas.1613144114 (2017).
173 Quarta, G. *et al.* Identifying the 993–994 CE Miyake event in the oldest dated living tree in Europe. *Radiocarbon* **61**, 1317-1325 (2019).
174 Park, J., Southon, J., Fahrni, S., Creasman, P. P. & Mewaldt, R. Relationship between solar activity and Δ14C peaks in AD 775, AD 994, and 660 BC. *Radiocarbon* **59**, 1147-1156, doi:10.1017/RDC.2017.59 (2017).
175 Dee, M. W. & Pope, B. J. Anchoring historical sequences using a new source of astro-chronological tie-points. *Proceedings of the Royal Society A: Mathematical, Physical and Engineering Sciences* **472**, 20160263 (2016).
176 Wacker, L. *et al.* Radiocarbon Dating to a Single Year by Means of Rapid Atmospheric C-14 Changes. *Radiocarbon* **56**, 573-579, doi:10.2458/56.17634 (2014).
177 Oppenheimer, C. *et al.* Multi-proxy dating the 'Millennium Eruption' of Changbaishan to late 946 CE. *Quaternary Science Reviews* **158**, 164-171 (2017).

178 Mazaud, A. *et al.* Geomagnetic-assisted stratigraphy and sea surface temperature changes in core MD94-103 (Southern Indian Ocean): possible implications for North-South climatic relationships around H4. *Earth and Planetary Science Letters* **201**, 159-170 (2002).
179 Cooper, A. *et al.* A global environmental crisis 42,000 years ago. *Science* **371**, 811-818 (2021).
180 Lister, A. M. & Stuart, A. J. The extinction of the giant deer Megaloceros giganteus (Blumenbach): New radiocarbon evidence. *Quaternary International* **500**, 185-203 (2019).
181 Kosintsev, P. *et al.* Evolution and extinction of the giant rhinoceros Elasmotherium sibiricum sheds light on late Quaternary megafaunal extinctions. *Nature ecology & evolution* **3**, 31-38 (2019).
182 Orlova, L. A., Kuzmin, Y. V. & Dementiev, V. N. A review of the evidence for extinction chronologies for five species of Upper Pleistocene megafauna in Siberia. *Radiocarbon* **46**, 301-314 (2004).
183 Roberts, R. G. *et al.* New ages for the last Australian megafauna: continent-wide extinction about 46,000 years ago. *Science* **292**, 1888-1892 (2001).
184 Miller, G. H. *et al.* Ecosystem collapse in Pleistocene Australia and a human role in megafaunal extinction. *science* **309**, 287-290 (2005).
185 Gillespie, R., Brook, B. W. & Baynes, A. Short overlap of humans and megafauna in Pleistocene Australia. *Alcheringa: An Australasian Journal of Palaeontology* **30**, 163-186 (2006).
186 Stewart, M., Carleton, W. C. & Groucutt, H. S. Climate change, not human population growth, correlates with Late Quaternary megafauna declines in North America. *Nature communications* **12**, 1-15 (2021).
187 Turnbull, J. C. *et al.* Sixty years of radiocarbon dioxide measurements at Wellington, New Zealand: 1954–2014. *Atmospheric Chemistry and Physics* **17**, 14771-14784 (2017).
188 Levin, I. & Kromer, B. The tropospheric (CO2)-C-14 level in mid-latitudes of the Northern Hemisphere (1959-2003). *Radiocarbon* **46**, 1261-1272 (2004).
189 Levin, I. *et al.* Observations and modelling of the global distribution and long-term trend of atmospheric 14CO2. *Tellus B: Chemical and Physical Meteorology* **62**, 26-46 (2010).
190 Hammer, S. & Levin, I. Monthly mean atmospheric D14CO2 at Jungfraujoch and Schauinsland from 1986 to 2016. *Tellus B* **65**, 20092 (2017).
191 Hua, Q. & Barbetti, M. Influence of atmospheric circulation on regional (CO2)-C-14 differences. *Journal of Geophysical Research-Atmospheres* **112**, - (2007).
192 Levin, I. & Hesshaimer, V. Radiocarbon - A unique tracer of global carbon cycle dynamics. *Radiocarbon* **42**, 69-80 (2000).
193 Hua, Q., Barbetti, M., Worbes, M., Head, J. & Levchenko, V. Review of radiocarbon data from atmospheric and tree ring samples for the period 1945-1997 AD. *Iawa Journal* **20**, 261-283 (1999).
194 Santos, G. M., Linares, R., Lisi, C. S. & Tomazello Filho, M. Annual growth rings in a sample of Paraná pine (Araucaria angustifolia): Toward improving the 14C calibration curve for the Southern Hemisphere. *Quaternary Geochronology* **25**, 96-103, doi:https://doi.org/10.1016/j.quageo.2014.10.004 (2015).
195 Ancapichún, S. *et al.* Radiocarbon bomb-peak signal in tree-rings from the tropical Andes register low latitude atmospheric dynamics in the Southern Hemisphere. *Science of the Total Environment* **774**, 145126 (2021).
196 Graven, H. D., Gruber, N., Key, R., Khatiwala, S. & Giraud, X. Changing controls on oceanic radiocarbon: New insights on shallow-to-deep ocean exchange and anthropogenic CO2 uptake. *Journal of Geophysical Research-Oceans* **117**, doi:Artn C10005 10.1029/2012jc008074 (2012).
197 Graven, H. D. Impact of fossil fuel emissions on atmospheric radiocarbon and various applications of radiocarbon over this century. *Proceedings of the National Academy of Sciences of the United States of America* **112**, 9542-9545, doi:10.1073/pnas.1504467112 (2015).

198 Levin, I., Hammer, S., Kromer, B. & Meinhardt, F. Radiocarbon observations in atmospheric CO2: Determining fossil fuel CO2 over Europe using Jungfraujoch observations as background. *Science of The Total Environment* **391**, 211-216 (2008).
199 Gamnitzer, U. *et al.* Carbon monoxide: A quantitative tracer for fossil fuel CO2? *Journal of Geophysical Research: Atmospheres* **111** (2006).
200 Graven, H., Hocking, T. & Zazzeri, G. Detection of fossil and biogenic methane at regional scales using atmospheric radiocarbon. *Earth's future* **7**, 283-299 (2019).
201 Xiong, X. *et al.* Time series of atmospheric Δ14CO2 recorded in tree rings from Northwest China (1957–2015). *Chemosphere* **272**, 129921, doi:https://doi.org/10.1016/j.chemosphere.2021.129921 (2021).
202 Szidat, S. *et al.* Contributions of fossil fuel, biomass-burning, and biogenic emissions to carbonaceous aerosols in Zurich as traced by 14C. *Journal of Geophysical Research: Atmospheres* **111** (2006).
203 Lim, S. *et al.* Fossil-driven secondary inorganic PM2. 5 enhancement in the North China Plain: Evidence from carbon and nitrogen isotopes. *Environmental Pollution* **266**, 115163 (2020).
204 Huang, L. *et al.* Application of the ECT9 protocol for radiocarbon-based source apportionment of carbonaceous aerosols. *Atmospheric Measurement Techniques* **14**, 3481-3500 (2021).
205 Dias, C. M. *et al.* 14CO2 dispersion around two PWR nuclear power plants in Brazil. *Journal of Environmental Radioactivity* **100**, 574-580, doi:https://doi.org/10.1016/j.jenvrad.2009.03.022 (2009).
206 Major, I. *et al.* Source identification of PM2.5 carbonaceous aerosol using combined carbon fraction, radiocarbon and stable carbon isotope analyses in Debrecen, Hungary. *Science of the Total Environment* **782**, doi:10.1016/j.scitotenv.2021.146520 (2021).
207 Pabedinskas, A. *et al.* Assessment of the Contamination by 14C Airborne Releases in the Vicinity of the Ignalina Nuclear Power Plant. *Radiocarbon* **61**, 1185-1197, doi:10.1017/RDC.2019.77 (2019).
208 Trumbore, S. Radiocarbon and soil carbon dynamics. *Annual Review of Earth and Planetary Sciences* **37**, 47-66 (2009).
209 Shi, Z. *et al.* The age distribution of global soil carbon inferred from radiocarbon measurements. *Nature Geoscience* **13**, 555-559 (2020).
210 Trumbore, S. E. & Zheng, S. Comparison of fractionation methods for soil organic matter 14C analysis. *Radiocarbon* **38**, 219-229 (1996).
211 Rethemeyer, J. *et al.* Transformation of organic matter in agricultural soils: radiocarbon concentration versus soil depth. *Geoderma* **128**, 94-105 (2005).
212 Hemingway, J. D. *et al.* Mineral protection regulates long-term global preservation of natural organic carbon. *Nature* **570**, 228-231 (2019).
213 Kuzyakov, Y., Bogomolova, I. & Glaser, B. Biochar stability in soil: decomposition during eight years and transformation as assessed by compound-specific 14C analysis. *Soil Biology and Biochemistry* **70**, 229-236 (2014).
214 Munksgaard, N. C. *et al.* Partitioning of microbially respired CO2 between indigenous and exogenous carbon sources during biochar degradation using radiocarbon and stable carbon isotopes. **61**, 573-586 (2019).
215 Estop-Aragonés, C. *et al.* Assessing the potential for mobilization of old soil carbon after permafrost thaw: A synthesis of 14C measurements from the northern permafrost region. *Global Biogeochemical Cycles* **34**, e2020GB006672 (2020).
216 Moore, S. *et al.* Deep instability of deforested tropical peatlands revealed by fluvial organic carbon fluxes. *Nature* **493**, 660-663 (2013).
217 Basu, S. *et al.* Estimating US fossil fuel CO2 emissions from measurements of 14C in atmospheric CO2. **117**, 13300-13307 (2020).
218 Cartwright, I., Currell, M. J., Cendón, D. I. & Meredith, K. T. A review of the use of radiocarbon to estimate groundwater residence times in semi-arid and arid areas. *Journal of Hydrology* **580**, 124247 (2020).

219 Hobbie, E. A., Weber, N. S., Trappe, J. M. & Van Klinken, G. J. Using radiocarbon to determine the mycorrhizal status of fungi. *New Phytologist* **156**, 129-136 (2002).

220 Newsham, K. K., Garnett, M. H., Robinson, C. H. & Cox, F. Discrete taxa of saprotrophic fungi respire different ages of carbon from Antarctic soils. *Scientific reports* **8**, 1-10 (2018).

221 Briones, M. a. J. I., Ineson, P. J. S. B. & Biochemistry. Use of 14C carbon dating to determine feeding behaviour of enchytraeids. **34**, 881-884 (2002).

222 Ishikawa, N. F. *et al.* Combined use of radiocarbon and stable carbon isotopes for the source mixing model in a stream food web. **65**, 2688-2696 (2020).

223 Wilson, S. A. *et al.* Assessing capture of atmospheric CO2 within mine tailings using stable isotopes and C-14. *Geochimica Et Cosmochimica Acta* **74**, A1135-A1135 (2010).

224 Wilson, S. A. *et al.* Offsetting of CO2 emissions by air capture in mine tailings at the Mount Keith Nickel Mine, Western Australia: Rates, controls and prospects for carbon neutral mining. *International Journal of Greenhouse Gas Control* **25**, 121-140 (2014).

225 Power, I. M. *et al.* Magnesite formation in playa environments near Atlin, British Columbia, Canada. *Geochimica Et Cosmochimica Acta* **255**, 1-24, doi:10.1016/j.gca.2019.04.008 (2019).

226 Broecker, W. S. & Peng, T.-H. *Tracers in the Sea*. 690 (Eldigio Press, 1982).

227 Broecker, W., Gerard, R., Ewing, M. & Heezen, B. C. Natural Radiocarbon in the Atlantic Ocean. *Journal of Geophysical Research* **65**, 2903-2931, doi:DOI 10.1029/JZ065i009p02903 (1960).

228 Druffel, E. M. Radiocarbon in annual coral rings from the eastern tropical Pacific Ocean. *Geophysical Research Letters* **8**, 59-62 (1981).

229 Nydal, R. Radiocarbon in the ocean. *Radiocarbon* **42**, 81-98 (2000).

230 Key, R. M. *et al.* A global ocean carbon climatology: Results from Global Data Analysis Project (GLODAP). *Global Biogeochemical Cycles* **18**, - (2004).

231 Guilderson, T. P., Caldeira, K. & Duffy, P. B. Radiocarbon as a diagnostic tracer in ocean and carbon cycle modeling. *Global Biogeochemical Cycles* **14**, 887-902 (2000).

232 Barker, S., Knorr, G., Vautravers, M. J., Diz, P. & Skinner, L. C. Extreme deepening of the Atlantic overturning circulation during deglaciation. *Nature Geoscience* **3**, 567-571 (2010).

233 Skinner, L. C., Fallon, S., Waelbroeck, C., Michel, E. & Barker, S. Ventilation of the deep Southern Ocean and deglacial CO2 rise. *Science* **328**, 1147-1151 (2010).

234 Walczak, M. H. *et al.* Phasing of millennial-scale climate variability in the Pacific and Atlantic Oceans. *Science* **370**, 716, doi:10.1126/science.aba7096 (2020).

235 Burke, A. & Robinson, L. F. The Southern Ocean's role in carbon exchange during the last deglaciation. *Science* **335**, 557-561 (2012).

236 Guilderson, T. P. & Schrag, D. P. Abrupt shift in subsurface temperatures in the tropical Pacific associated with changes in El Niño. *Science* **281**, 240-243 (1998).

237 McNichol, A. P. & Aluwihare, L. I. The power of radiocarbon in biogeochemical studies of the marine carbon cycle: Insights from studies of dissolved and particulate organic carbon (DOC and POC). *Chemical reviews* **107**, 443-466 (2007).

238 Williams, P. M. & Druffel, E. R. Radiocarbon in dissolved organic matter in the central North Pacific Ocean. *Nature* **330**, 246-248 (1987).

239 Bauer, J. E., Williams, P. M. & Druffel, E. R. 14 C activity of dissolved organic carbon fractions in the north-central Pacific and Sargasso Sea. *Nature* **357**, 667-670 (1992).

240 Druffel, E. R. & Bauer, J. E. Radiocarbon distributions in Southern Ocean dissolved and particulate organic matter. *Geophysical research letters* **27**, 1495-1498 (2000).

241 Ishikawa, N. F., Butman, D. & Raymond, P. A. Radiocarbon age of different photoreactive fractions of freshwater dissolved organic matter. *Organic Geochemistry* **135**, 11-15, doi:https://doi.org/10.1016/j.orggeochem.2019.06.006 (2019).

242 Beaupré, S. R., Walker, B. D. & Druffel, E. R. M. The two-component model coincidence: Evaluating the validity of marine dissolved organic radiocarbon as a stable-conservative tracer at Station M. *Deep Sea Research Part II: Topical Studies in Oceanography* **173**, 104737, doi:https://doi.org/10.1016/j.dsr2.2020.104737 (2020).

243 Druffel, E. R. & Williams, P. M. Identification of a deep marine source of particulate organic carbon using bomb 14 C. *Nature* **347**, 172-174 (1990).
244 Druffel, E. R., Bauer, J. E., Griffin, S. & Hwang, J. Penetration of anthropogenic carbon into organic particles of the deep ocean. *Geophysical research letters* **30** (2003).
245 Verdugo, P. *et al.* The oceanic gel phase: a bridge in the DOM–POM continuum. *Marine Chemistry* **92**, 67-85 (2004).
246 Spalding, K. L., Bhardwaj, R. D., Buchholz, B. A., Druid, H. & Frisen, J. Retrospective birth dating of cells in humans. *Cell* **122**, 133-143, doi:10.1016/j.cell.2005.04.028 (2005).
247 Bergmann, O. *et al.* The age of olfactory bulb neurons in humans. *Neuron* **74**, 634-639 (2012).
248 Bhardwaj, R. D. *et al.* Neocortical neurogenesis in humans is restricted to development. *Proceedings of the National Academy of Sciences* **103**, 12564-12568 (2006).
249 Huttner, H. B. *et al.* The age and genomic integrity of neurons after cortical stroke in humans. *Nature neuroscience* **17**, 801-803 (2014).
250 Spalding, K. L. *et al.* Dynamics of hippocampal neurogenesis in adult humans. *Cell* **153**, 1219-1227 (2013).
251 Ernst, A. *et al.* Neurogenesis in the striatum of the adult human brain. *Cell* **156**, 1072-1083 (2014).
252 Yeung, M. S. *et al.* Dynamics of oligodendrocyte generation and myelination in the human brain. *Cell* **159**, 766-774 (2014).
253 Réu, P. *et al.* The lifespan and turnover of microglia in the human brain. *Cell reports* **20**, 779-784 (2017).
254 Bergmann, O. *et al.* Evidence for cardiomyocyte renewal in humans. *Science* **324**, 98-102 (2009).
255 Bergmann, O. *et al.* Dynamics of cell generation and turnover in the human heart. *Cell* **161**, 1566-1575 (2015).
256 Spalding, K. L. *et al.* Dynamics of fat cell turnover in humans. *Nature* **453**, 783-787 (2008).
257 Huttner, H. B. *et al.* Meningioma growth dynamics assessed by radiocarbon retrospective birth dating. *Ebiomedicine* **27**, 176-181 (2018).
258 Mold, J. E. *et al.* Cell generation dynamics underlying naive T-cell homeostasis in adult humans. *PLoS Biology* **17**, e3000383 (2019).
259 Arner, P. *et al.* Dynamics of human adipose lipid turnover in health and metabolic disease. *Nature* **478**, 110-113, doi:10.1038/nature10426 (2011).
260 Spalding, K. L. *et al.* Impact of fat mass and distribution on lipid turnover in human adipose tissue. *Nature communications* **8**, 1-9 (2017).
261 Arner, P. *et al.* Adipose lipid turnover and long-term changes in body weight. *Nature medicine* **25**, 1385-1389 (2019).
262 Libby, W. F. Radiocarbon Dates .2. *Science* **114**, 291-296 (1951).
263 Jull, A. J. T. *et al.* Radiocarbon Dating and Intercomparison of Some Early Historical Radiocarbon Samples. *Radiocarbon* **60**, 535-548, doi:10.1017/Rdc.2018.18 (2018).
264 Kasso, T. M., Oinonen, M. J., Mizohata, K., Tahkokallio, J. K. & Heikkilä, T. M. Volumes of Worth—Delimiting the Sample Size for Radiocarbon Dating of Parchment. *Radiocarbon* **63**, 105-120 (2021).
265 Brock, F. Radiocarbon dating of historical parchments. *Radiocarbon* **55**, 353-363 (2013).
266 Brock, F., Ostapkowicz, J., Wiedenhoeft, A. C. & Bull, I. D. Radiocarbon Dating Wooden Carvings and Skeletal Remains from Pitch Lake, Trinidad. *Radiocarbon* **59**, 1447-1461, doi:10.1017/RDC.2017.78 (2017).
267 Liccioli, L., Fedi, M., Carraresi, L. & Mando, P. A. Characterization of the Chloroform-Based Pretreatment Method for C-14 Dating of Restored Wooden Samples. *Radiocarbon* **59**, 757-764, doi:10.1017/Rdc.2016.83 (2017).
268 Solís, C. *et al.* Ams 14C dating of the mayan codex of mexico revisited. *Radiocarbon* **62**, 1543-1550 (2020).

269 Ringbom, A., Lindroos, A., Heinemeier, J. & Sonck-Koota, P. 19 Years of Mortar Dating: Learning from Experience. *Radiocarbon* **56**, 619-635, doi:Doi 10.2458/56.17469 (2014).
270 Urbanová, P., Boaretto, E. & Artioli, G. The State-of-the-Art of Dating Techniques Applied to Ancient Mortars and Binders: A Review. *Radiocarbon* **62**, 503-525, doi:10.1017/RDC.2020.43 (2020).
271 Michalska, D., Czernik, J. & Goslar, T. Methodological aspect of mortars dating (Poznań, Poland, MODIS). *Radiocarbon* **59**, 1891-1906 (2017).
272 Caroselli, M., Hajdas, I. & Cassitti, P. Radiocarbon Dating of Dolomitic Mortars from the Convent Saint John, Müstair (Switzerland): First Results. *Radiocarbon* **62**, 601-615, doi:10.1017/RDC.2020.35 (2020).
273 Barrett, G. T. *et al.* Ramped pyroxidation: A new approach for radiocarbon dating of lime mortars. *Journal of Archaeological Science* **129**, 105366 (2021).
274 Derrick, M. R., Stulik, D. & Landry, J. M. *Infrared spectroscopy in conservation science*. (Getty Publications, 2000).
275 Ford, T., Rizzo, A., Hendriks, E., Frøysaker, T. & Caruso, F. A non-invasive screening study of varnishes applied to three paintings by Edvard Munch using portable diffuse reflectance infrared Fourier transform spectroscopy (DRIFTS). *Heritage Science* **7**, 1-13 (2019).
276 Vitali, F. *et al.* The vernacular sculpture of Saint Anthony the Abbot of Museo Colle del Duomo in Viterbo (Italy). Diagnostic and Wood dating. *Journal of Cultural Heritage* **48**, 299-304, doi:https://doi.org/10.1016/j.culher.2021.01.006 (2021).
277 Colombini, M. P. & Modugno, F. *Organic mass spectrometry in art and archaeology*. (John Wiley & Sons, 2009).
278 Hendriks, L. *et al.* Microscale radiocarbon dating of paintings. *Applied Physics A* **122**, doi:10.1007/s00339-016-9593-x (2016).
279 Quarta, G., D'Elia, M., Paparella, S., Serra, A. & Calcagnile, L. Characterisation of lead carbonate white pigments submitted to AMS radiocarbon dating. *Journal of Cultural Heritage* **46**, 102-107 (2020).
280 Fiorillo, F., Hendriks, L., Hajdas, I., Vandini, M. & Huysecom, E. The Rediscovery of Jan Ruyscher and Its Consequence. *J Am Inst Conserv*, doi:10.1080/01971360.2020.1822702 (2021).
281 Hajdas, I. *et al.* Bomb C-14 on Paper and Detection of the Forged Paintings of T'ang Haywen. *Radiocarbon* **61**, 1905-1912, doi:10.1017/Rdc.2019.120 (2019).
282 Hüls, M., Grootes, P. M. & Nadeau, M.-J. Sampling iron for radiocarbon dating: influence of modern steel tools on 14C dating of ancient iron artifacts. *Radiocarbon* **53**, 151-160 (2011).
283 Claggett, D. *et al.* Modern or medieval? Analysis of an iron anchor from Camuscross, Scotland and direct dating methods for metal artefacts. *Journal of Archaeological Science: Reports* **25**, 144-152 (2019).
284 Hüls, C. M., Petri, I. & Föll, H. Absolute Dating of Early Iron Objects from the Ancient Orient: Radiocarbon Dating of Luristan Iron Mask Swords. *Radiocarbon* **61**, 1229-1238 (2019).
285 Durier, M. *et al.* Radiocarbon dating of legacy music instrument collections: Example of traditional indian Vina from the Musée De La Musique, Paris. *Radiocarbon* **61**, 1357-1366 (2019).
286 Patrut, A. *et al.* The demise of the largest and oldest African baobabs. *Nature Plants* **4**, 423-426, doi:10.1038/s41477-018-0170-5 (2018).
287 Patrut, A. *et al.* African Baobabs with False Inner Cavities: The Radiocarbon Investigation of the Lebombo Eco Trail Baobab. *Plos One* **10**, doi:ARTN e0117193 10.1371/journal.pone.0117193 (2015).
288 Patrut, A. *et al.* The Growth Stop Phenomenon of Baobabs (Adansonia Spp.) Identified by Radiocarbon Dating. *Radiocarbon* **59**, 435-448, doi:10.1017/Rdc.2016.92 (2017).
289 Piovesan, G. *et al.* Dating old hollow trees by applying a multistep tree-ring and radiocarbon procedure to trunk and exposed roots. *MethodsX* **5**, 495-502 (2018).
290 Wild, E. M. First 14C results from archaeological and forensic studies at the Vienna Environmental Research Accelerator. *Radiocarbon* **40**, 273-281 (1998).

291 Jørkov, M. L. S., Heinemeier, J. & Lynnerup, N. The petrous bone—A new sampling site for identifying early dietary patterns in stable isotopic studies. *American journal of physical anthropology* **138**, 199-209 (2009).
292 Spalding, K. L., Buchholz, B. A., Bergman, L. E., Druid, H. & Frisen, J. Forensics: age written in teeth by nuclear tests. *Nature* **437**, 333-334, doi:10.1038/437333a (2005).
293 Speller, C. F. *et al.* Personal Identification of Cold Case Remains Through Combined Contribution from Anthropological, mt DNA, and Bomb-Pulse Dating Analyses. *J Forensic Sci* **57**, 1354-1360 (2012).
294 Alkass, K., Buchholz, B., Druid, H. & Spalding, K. Analysis of 14C and 13C in teeth provides precise birth dating and clues to geographical origin. *Forensic science international* **209**, 34-41 (2011).
295 Alkass, K. *et al.* Age estimation in forensic sciences: application of combined aspartic acid racemization and radiocarbon analysis. *Molecular & Cellular Proteomics* **9**, 1022-1030 (2010).
296 Cook, G. T., Dunbar, E., Black, S. M. & Xu, S. A preliminary assessment of age at death determination using the nuclear weapons testing 14C activity of dentine and enamel. *Radiocarbon* **48**, 305-313 (2006).
297 Buchholz, B. & Spalding, K. Year of birth determination using radiocarbon dating of dental enamel. *Surface and Interface Analysis: An International Journal devoted to the development and application of techniques for the analysis of surfaces, interfaces and thin films* **42**, 398-401 (2010).
298 Alkass, K. *et al.* Analysis of radiocarbon, stable isotopes and DNA in teeth to facilitate identification of unknown decedents. *PLoS One* **8**, e69597 (2013).
299 Saitoh, H. *et al.* Estimation of birth year by radiocarbon dating of tooth enamel: Approach to obtaining enamel powder. *Journal of forensic and legal medicine* **62**, 97-102 (2019).
300 Kjeldsen, H., Heinemeier, J., Heegaard, S., Jacobsen, C. & Lynnerup, N. Dating the time of birth: A radiocarbon calibration curve for human eye-lens crystallines. *Nuclear Instruments & Methods in Physics Research Section B-Beam Interactions with Materials and Atoms* **268**, 1303-1306, doi:10.1016/j.nimb.2009.10.158 (2010).
301 Lynnerup, N., Kjeldsen, H., Heegaard, S., Jacobsen, C. & Heinemeier, J. Radiocarbon Dating of the Human Eye Lens Crystallines Reveal Proteins without Carbon Turnover throughout Life. *Plos One* **3**, doi:ARTN e1529 10.1371/journal.pone.0001529 (2008).
302 Uno, K. T. *et al.* Bomb-curve radiocarbon measurement of recent biologic tissues and applications to wildlife forensics and stable isotope (paleo)ecology. *Proceedings of the National Academy of Sciences* **110**, 11736, doi:10.1073/pnas.1302226110 (2013).
303 Cerling, T. E. *et al.* Radiocarbon dating of seized ivory confirms rapid decline in African elephant populations and provides insight into illegal trade. *Proceedings of the National Academy of Sciences of the United States of America* **113**, 13330-13335, doi:10.1073/pnas.1614938113 (2016).
304 Schmidberger, A., Durner, B., Gehrmeyer, D. & Schupfner, R. Development and application of a method for ivory dating by analyzing radioisotopes to distinguish legal from illegal ivory. *Forensic science international* **289**, 363-367 (2018).
305 Quarta, G., D'Elia, M., Braione, E. & Calcagnile, L. Radiocarbon dating of ivory: Potentialities and limitations in forensics. *Forensic science international* **299**, 114-118 (2019).
306 Wild, E. M., Kutschera, W., Meran, A. & Steier, P. 14 C Bomb Peak Analysis of African Elephant Tusks and its Relation to Cites. *Radiocarbon* **61**, 1619-1624 (2019).
307 Dormontt, E. E. *et al.* Forensic timber identification: It's time to integrate disciplines to combat illegal logging. *Biol Conserv* **191**, 790-798 (2015).
308 Lowe, A. J. *et al.* Opportunities for improved transparency in the timber trade through scientific verification. *BioScience* **66**, 990-998 (2016).
309 Retief, K., West, A. G. & Pfab, M. F. Can stable isotopes and radiocarbon dating provide a forensic solution for curbing illegal harvesting of threatened cycads? *J Forensic Sci* **59**, 1541-1551 (2014).

310 Köhler, P. Using the Suess effect on the stable carbon isotope to distinguish the future from the past in radiocarbon. *Environ Res Lett* **11**, 124016 (2016).
311 Quarta, G., Calcagnile, L., Giffoni, M., Braione, E. & D'Elia, M. Determination of the biobased content in plastics by radiocarbon. *Radiocarbon* **55**, 1834-1844 (2013).
312 Dijs, I. J., Van der Windt, E., Kaihola, L. & van der Borg, K. Quantitative determination by 14C analysis of the biological component in fuels. *Radiocarbon* **48**, 315-323 (2006).
313 Varga, T. *et al.* High-Precision Biogenic Fraction Analyses of Liquid Fuels by 14 C AMS at HEKAL. *Radiocarbon* **60**, 1317-1325 (2018).
314 Palstra, S. W. L., Rabou, L. P. L. M. & Meijer, H. A. J. Radiocarbon-based determination of biogenic and fossil carbon partitioning in the production of synthetic natural gas. *Fuel* **157**, 177-182, doi:https://doi.org/10.1016/j.fuel.2015.04.076 (2015).
315 Calcagnile, L., Quarta, G., D'Elia, M., Ciceri, G. & Martinotti, V. Radiocarbon AMS determination of the biogenic component in CO2 emitted from waste incineration. *Nuclear Instruments and Methods in Physics Research Section B: Beam Interactions with Materials and Atoms* **269**, 3158-3162 (2011).
316 Quarta, G. *et al.* AMS-14 C determination of the biogenic-fossil fractions in flue gases. *Radiocarbon* **60**, 1327-1333 (2018).
317 Bronić, I. K., Barešić, J., Horvatinčić, N. & Sironić, A. Determination of biogenic component in liquid fuels by the 14C direct LSC method by using quenching properties of modern liquids for calibration. *Radiation Physics and Chemistry* **137**, 248-253 (2017).
318 13833:2013, I. Stationary source emissions – Determination of the ratio of biomass (biogenic) and fossil-derived carbon dioxide – Radiocarbon sampling and determination.
319 D6866, A. M. Standard Test Methods for Determining the Biobased Content of Solid, Liquid, and Gaseous Samples Using Radiocarbon Analysis.
320 Nilsson, M. *et al.* Analysis of the Putative Remains of a European Patron Saint–St. Birgitta. *PLOS ONE* **5**, e8986, doi:10.1371/journal.pone.0008986 (2010).
321 Damon, P. E. *et al.* Radiocarbon Dating of the Shroud of Turin. *Nature* **337**, 611-615 (1989).
322 De Vries, H. & Oakley, K. P. Radiocarbon Dating of the Piltdown Skull and Jaw. *Nature* **184**, 224-226, doi:10.1038/184224a0 (1959).
323 De Groote, I. *et al.* New genetic and morphological evidence suggests a single hoaxer created ‘Piltdown man&#x2019. *Royal Society Open Science* **3**, 160328, doi:doi:10.1098/rsos.160328 (2016).
324 Caforio, L. *et al.* Discovering forgeries of modern art by the C-14 Bomb Peak. *European Physical Journal Plus* **129**, doi:10.1140/epjp/i2014-14006-6 (2014).
325 Petrucci, F. *et al.* Radiocarbon dating of twentieth century works of art. *Applied Physics A* **122**, 983 (2016).
326 Hendriks, L. *et al.* Uncovering modern paint forgeries by radiocarbon dating. *Proceedings of the National Academy of Sciences* **116**, 13210-13214, doi:10.1073/pnas.1901540116 (2019).
327 Olsson, I. U. Radiocarbon Dating History: Early Days, Questions, and Problems Met. *Radiocarbon* **51**, 1-43 (2009).
328 Scott, E. M., Cook, G. T. & Naysmith, P. The Fifth International Radiocarbon Intercomparison (VIRI): an assessment of laboratory performance in stage 3. *Radiocarbon* **52**, 859-865 (2010).
329 Naysmith, P. *et al.* A cremated bone intercomparison study. *Radiocarbon* **49**, 403-408 (2007).
330 Kuzmin, Y. V. *et al.* A laboratory inter-comparison of AMS14C dating of bones of the Miesenheim IV elk (Rhineland, Germany) and its implications for the date of the Laacher See eruption. (2018).
331 Scott, E., Cook, G., Naysmith, P. & Staff, R. Learning from the wood samples in ICS, TIRI, FIRI, VIRI and SIRI. *Radiocarbon* **61**, 1293-1304 (2019).
332 Quiles, A. *et al.* Second Radiocarbon Intercomparison Program for the Chauvet-Pont D'arc Cave, Ardeche, France. *Radiocarbon* **56**, 833-850, doi:10.2458/56.16940 (2014).
333 Millard, A. R. Conventions for Reporting Radiocarbon Determinations. *Radiocarbon* **56**, 555-559, doi:10.2458/56.17455 (2014).

334 Bayliss, A. Quality in Bayesian chronological models in archaeology. *World Archaeol* **47**, 677-700 (2015).
335 Johnson, F. Radiocarbon Dating Lists and Their Use. *American Antiquity* **21**, 312-313, doi:10.2307/277210 (1956).
336 Johnson, F. J. R. A Bibliography of Radiocarbon Dating∗. **1**, 199-214 (1959).
337 Hedges, R., Housley, R., Ramsey, C. B. & Van Klinken, G. J. A. Radiocarbon dates from the Oxford AMS system: Archaeometry datelist 18. **36**, 337-374 (1994).
338 Broecker, W. S., Kulp, J. L. & Tucek, C. S. Lamont Natural Radiocarbon Measurements .3. *Science* **124**, 154-165, doi:DOI 10.1126/science.124.3213.154 (1956).
339 Olson, E. A. & Broecker, W. S. Lamont Natural Radiocarbon Measurements .5. *American Journal of Science* **257**, 1-28, doi:DOI 10.2475/ajs.257.1.1 (1959).
340 Broecker, W. S. & Olson, E. A. Lamont radiocarbon measurements VIII. *Radiocarbon* **3**, 176-204 (1961).
341 Vermeersch, P. M. Radiocarbon Palaeolithic Europe database: A regularly updated dataset of the radiometric data regarding the Palaeolithic of Europe, Siberia included. *Data Brief* **31**, 105793-105793, doi:10.1016/j.dib.2020.105793 (2020).
342 Loftus, E., Mitchell, P. J. & Ramsey, C. B. An archaeological radiocarbon database for southern Africa. *Antiquity* **93**, 870-885, doi:10.15184/aqy.2019.75 (2019).
343 Gajewski, K. *et al.* The Canadian Archaeological Radiocarbon Database (Card): Archaeological 14C Dates in North America and Their Paleoenvironmental Context. *Radiocarbon* **53**, 371-394, doi:10.1017/S0033822200056630 (2011).
344 Bryson, R., Bryson, R. & Ruter, A. A calibrated radiocarbon database of late Quaternary volcanic eruptions. *eEarth Discussions* **1**, 123-134 (2006).
345 Lawrence, C. R. *et al.* An open-source database for the synthesis of soil radiocarbon data: International Soil Radiocarbon Database (ISRaD) version 1.0. *Earth Syst. Sci. Data* **12**, 61-76, doi:10.5194/essd-12-61-2020 (2020).
346 Herrando-Pérez, S. Bone need not remain an elephant in the room for radiocarbon dating. *Royal Society Open Science* **8**, 201351, doi:doi:10.1098/rsos.201351 (2021).
347 van der Voort, T. S. *et al.* MOSAIC (Modern Ocean Sediment Archive and Inventory of Carbon): a (radio)carbon-centric database for seafloor surficial sediments. *Earth Syst. Sci. Data* **13**, 2135-2146, doi:10.5194/essd-13-2135-2021 (2021).
348 Sánchez Goñi, M. F. *et al.* The ACER pollen and charcoal database: a global resource to document vegetation and fire response to abrupt climate changes during the last glacial period. *Earth Syst. Sci. Data* **9**, 679-695, doi:10.5194/essd-9-679-2017 (2017).
349 Guilderson, T. P., Reimer, P. J. & Brown, T. A. The boon and bane of radiocarbon dating. *Science* **307**, 362-364 (2005).
350 Svetlik, I. *et al.* The best possible time resolution: how precise could a radiocarbon dating method be? *Radiocarbon* **61**, 1729-1740 (2019).
351 Ramsey, C. B., van der Plicht, J. & Weninger, B. 'Wiggle matching' radiocarbon dates. *Radiocarbon* **43**, 381-389 (2001).
352 Mol, D. *et al.* Results of the CERPOLEX/Mammuthus Expeditions on the Taimyr Peninsula, Arctic Siberia, Russian Federation. *Quaternary International* **142-143**, 186-202, doi:https://doi.org/10.1016/j.quaint.2005.03.016 (2006).
353 Maruccio, L., Quarta, G., Braione, E. & Calcagnile, L. Measuring stable carbon and nitrogen isotopes by IRMS and 14C by AMS on samples with masses in the microgram range: performances of the system installed at CEDAD-University of Salento. *Int J Mass Spectrom* **421**, 1-7 (2017).
354 McIntyre, C. P. *et al.* Online C-13 and C-14 Gas Measurements by Ea-Irms-Ams at Eth Zurich. *Radiocarbon* **59**, 893-903, doi:10.1017/Rdc.2016.68 (2017).
355 Blattmann, T. M. & Ishikawa, N. F. Theoretical amino acid-specific radiocarbon content in the environment: Hypotheses to be tested and opportunities to be taken. *Current Topics in Marine Organic Biogeochemical Research* (2021).

356 Deviese, T., Comeskey, D., McCullagh, J., Bronk Ramsey, C. & Higham, T. New protocol for compound-specific radiocarbon analysis of archaeological bones. *Rapid Communications in Mass Spectrometry* **32**, 373-379 (2018).
357 Hamady, L. L., Natanson, L. J., Skomal, G. B. & Thorrold, S. R. Vertebral Bomb Radiocarbon Suggests Extreme Longevity in White Sharks. *PLOS ONE* **9**, e84006, doi:10.1371/journal.pone.0084006 (2014).
358 Nielsen, J. *et al.* Eye lens radiocarbon reveals centuries of longevity in the Greenland shark (Somniosus microcephalus). *Science* **353**, 702-704 (2016).
359 Loader, N. J. *et al.* Tree ring dating using oxygen isotopes: a master chronology for central England. *Journal of Quaternary Science* **34**, 475-490 (2019).
360 Sigl, M. *et al.* Timing and climate forcing of volcanic eruptions for the past 2,500 years. *Nature* **523**, 543-549 (2015).
361 Brehm, N. *et al.* Eleven-year solar cycles over the last millennium revealed by radiocarbon in tree rings. *Nature Geoscience* **14**, 10-15, doi:10.1038/s41561-020-00674-0 (2021).
362 Land, A., Kromer, B., Remmele, S., Brehm, N. & Wacker, L. Complex imprint of solar variability on tree rings. *Environmental Research Communications* **2**, 101003 (2020).
363 Libby, W. F. Half-life of radiocarbon. *Radiocarbon dating*, 34–42 (1952).
364 Godwin, H. Half-Life of Radiocarbon. *Nature* **195**, 984-& (1962).
365 Buck, C. E. & Sahu, S. K. Bayesian models for relative archaeological chronology building. *Journal of the Royal Statistical Society Series C-Applied Statistics* **49**, 423-440 (2000).
366 Ramsey, C. B. Deposition models for chronological records. *Quaternary Science Reviews* **27**, 42-60 (2008).
367 Hajdas, I., Sojc, U., Ivy-Ochs, S., Akçar, N. & Deline, P. Radiocarbon Dating for the Reconstruction of the 1717 CE Triolet Rock Avalanche in the Mont Blanc Massif, Italy. *Frontiers in Earth Science* **8**, doi:10.3389/feart.2020.580293 (2021).
368 Yamamoto, S. *et al.* Compound-Specific Radiocarbon Analysis of Organic Compounds from Mount Fuji Proximal Lake (Lake Kawaguchi) Sediment, Central Japan. *Radiocarbon* **62**, 439-451, doi:10.1017/RDC.2019.158 (2020).
369 Gierga, M. *et al.* Long-stored soil carbon released by prehistoric land use: evidence from compound-specific radiocarbon analysis on Soppensee lake sediments. *Quaternary Science Reviews* **144**, 123-131 (2016).
370 Heinemeier, K. M., Schjerling, P., Heinemeier, J., Magnusson, S. P. & Kjaer, M. Lack of tissue renewal in human adult Achilles tendon is revealed by nuclear bomb 14C. *The FASEB Journal* **27**, 2074-2079 (2013).
371 Heinemeier, K. M. *et al.* Radiocarbon dating reveals minimal collagen turnover in both healthy and osteoarthritic human cartilage. *Science Translational Medicine* **8**, 346ra390-346ra390, doi:10.1126/scitranslmed.aad8335 (2016).
372 Ubelaker, D. H. Radiocarbon Analysis of Human Remains: A Review of Forensic Applications. *J Forensic Sci* **59**, 1466-1472, doi:https://doi.org/10.1111/1556-4029.12535 (2014).
373 Castro, K. *et al.* Multianalytical approach to the analysis of English polychromed alabaster sculptures: µRaman, µEDXRF, and FTIR spectroscopies. *Analytical and Bioanalytical Chemistry* **392**, 755-763, doi:10.1007/s00216-008-2317-0 (2008).
374 Casadio, F., Daher, C. & Bellot-Gurlet, L. in *Analytical Chemistry for Cultural Heritage* (ed Rocco Mazzeo) 161-211 (Springer International Publishing, 2017).
375 Švarcová, S., Kočí, E., Bezdička, P., Hradil, D. & Hradilová, J. Evaluation of laboratory powder X-ray micro-diffraction for applications in the fields of cultural heritage and forensic science. *Analytical and Bioanalytical Chemistry* **398**, 1061-1076, doi:10.1007/s00216-010-3980-5 (2010).
376 Marzaioli, F. *et al.* Characterisation of a new protocol for mortar dating: 14C evidences. *Open Journal of Archaeometry* **2** (2014).
377 Yates, T. Studies of non-marine mollusks for the selection of shell samples for radiocarbon dating. *Radiocarbon* **28**, 457-463 (1986).

378 D'Elia, M. *et al.* Evaluation of possible contamination sources in the C-14 analysis of bone samples by FTIR spectroscopy. *Radiocarbon* **49**, 201-210 (2007).
379 Gianfrate, G. *et al.* Qualitative application based on IR spectroscopy for bone sample quality control in radiocarbon dating. *Nuclear Instruments and Methods in Physics Research Section B: Beam Interactions with Materials and Atoms*
Accelerator Mass Spectrometry - Proceedings of the Tenth International Conference on Accelerator Mass Spectrometry **259**, 316-319 (2007).
380 Zazzo, A., Saliège, J.-F., Person, A. & Boucher, H. Radiocarbon dating of calcined bones: Where does the carbon come from? *Radiocarbon* **51**, 601-611 (2009).
381 Alon, D., Mintz, G., Cohen, I., Weiner, S. & Boaretto, E. The use of Raman spectroscopy to monitor the removal of humic substances from charcoal: quality control for 14C dating of charcoal. *Radiocarbon* **44**, 1-11 (2002).
382 Ospitali, F., Smith, D. C. & Lorblanchet, M. Preliminary investigations by Raman microscopy of prehistoric pigments in the wall-painted cave at Roucadour, Quercy, France. *Journal of Raman Spectroscopy: An International Journal for Original Work in all Aspects of Raman Spectroscopy, Including Higher Order Processes, and also Brillouin and Rayleigh Scattering* **37**, 1063-1071 (2006).
383 Boaretto, E. *et al.* Radiocarbon dating of charcoal and bone collagen associated with early pottery at Yuchanyan Cave, Hunan Province, China. *Proceedings of the National Academy of Sciences* **106**, 9595-9600 (2009).
384 Lahlil, S. *et al.* The first in situ micro-Raman spectroscopic analysis of prehistoric cave art of Rouffignac St-Cernin, France. *Journal of Raman Spectroscopy* **43**, 1637-1643 (2012).
385 Hendriks, L. *et al.* Microscale radiocarbon dating of paintings. *Applied Physics a-Materials Science & Processing* **122**, doi:ARTN 167
10.1007/s00339-016-9593-x (2016).
386 Hendriks, L. *et al.* Uncovering modern paint forgeries by radiocarbon dating. *Proc Natl Acad Sci U S A* **116**, 13210-13214, doi:10.1073/pnas.1901540116 (2019).
387 Hendriks, L. *et al.* Selective Dating of Paint Components: Radiocarbon Dating of Lead White Pigment. *Radiocarbon* **61**, 473-493, doi:10.1017/Rdc.2018.101 (2019).
388 Bird, M., Ascough, P., Young, I., Wood, C. & Scott, A. X-ray microtomographic imaging of charcoal. *Journal of Archaeological Science* **35**, 2698-2706, doi:10.1016/j.jas.2008.04.018 (2008).
389 Huang, Y., Li, B., Bryant, C., Bol, R. & Eglinton, G. Radiocarbon Dating of Aliphatic Hydrocarbons A New Approach for Dating Passive-Fraction Carbon in Soil Horizons. *Soil Science Society of America Journal* **63**, 1181-1187 (1999).
390 Santos, G., De La Torre, H., Boudin, M., Bonafini, M. & Saverwyns, S. Improved radiocarbon analyses of modern human hair to determine the year-of-death by cross-flow nanofiltered amino acids: common contaminants, implications for isotopic analysis, and recommendations. *Rapid Communications in Mass Spectrometry* **29**, 1765-1773, doi:10.1002/rcm.7273 (2015).
391 Van Strydonck, M. *et al.* 14C-dating of the skeleton remains and the content of the lead coffin attributed to the Blessed Idesbald (Abbey of the Dunes, Koksijde, Belgium). *Journal of Archaeological Science: Reports* **5**, 276-284 (2016).
392 Teetaert, D., Boudin, M., Saverwyns, S. & Crombé, P. Food and soot: organic residues on outer pottery surfaces. *Radiocarbon* **59**, 1609 (2017).
393 Cersoy, S., Daheur, G., Zazzo, A., Zirah, S. & Sablier, M. Pyrolysis comprehensive gas chromatography and mass spectrometry: A new tool to assess the purity of ancient collagen prior to radiocarbon dating. *Anal Chim Acta* **1041**, 131-145, doi:10.1016/j.aca.2018.07.048 (2018).
394 Wagner, T. V. *et al.* Molecular characterization of charcoal to identify adsorbed SOM and assess the effectiveness of common SOM-removing pretreatments prior to radiocarbon dating. *Quaternary Geochronology* **45**, 74-84 (2018).

395 Casanova, E., Knowles, T. D., Williams, C., Crump, M. P. & Evershed, R. P. Use of a 700 MHz NMR microcryoprobe for the identification and quantification of exogenous carbon in compounds purified by preparative capillary gas chromatography for radiocarbon determinations. *Analytical chemistry* **89**, 7090-7098 (2017).
396 Boudin, M., Boeckx, P., Vandenabeele, P., Mitschke, S. & Strydonck, M. V. A. N. Monitoring the presence of humic substances in wool and silk by the use of nondestructive fluorescence spectroscopy: quality control for 14 C dating of wool and silk. *Radiocarbon* **53**, 429–442 (2011).
397 Bird, M. I. *et al.* Radiocarbon dating of "old" charcoal using a wet oxidation, stepped-combustion procedure. *Radiocarbon* **41**, 127-140 (1999).
398 Broecker, W. S. & Farrand, W. R. Radiocarbon age of the Two Creeks forest bed, Wisconsin. *Geological Society of America Bulletin* **74**, 795-802 (1963).
399 Nemec, M., Wacker, L., Hajdas, I. & Gaggeler, H. Alternative Methods for Cellulose Preparation for Ams Measurement. *Radiocarbon* **52**, 1358-1370 (2010).
400 Czimczik, C. I., Trumbore, S. E., Xu, X., Carbone, M. S. & Richardson, A. D. Extraction of nonstructural carbon and cellulose from wood for radiocarbon analysis. *Bio-protocol* **4**, e1169-e1169 (2014).
401 Hajdas, I., Hendriks, L., Fontana, A. & Monegato, G. Evaluation of Preparation Methods in Radiocarbon Dating of Old Woods. *Radiocarbon* **59**, 727-737 (2017).
402 Eglinton, T. I. *et al.* Compound specific radiocarbon analysis as a tool to quantitatively apportion modern and fossil sources of polycyclic aromatic hydrocarbons in environmental matrices. *Abstracts of Papers of the American Chemical Society* **212**, 65-ENVR (1996).
403 Dahl, K. A. *et al.* Terrigenous plant wax inputs to the Arabian Sea: Implications for the reconstruction of winds associated with the Indian Monsoon. *Geochimica et Cosmochimica Acta* **69**, 2547-2558 (2005).
404 Ohkouchi, N., Eglinton, T., Hughen, K., Roosen, E. & Keigwin, L. Radiocarbon dating of alkenones from marine sediments: III. Influence of solvent extraction procedures on C-14 measurements of foraminifera. *Radiocarbon* **47**, 425-432 (2005).
405 Sun, S. W. *et al.* C-14 Blank Assessment in Small-Scale Compound-Specific Radiocarbon Analysis of Lipid Biomarkers and Lignin Phenols. *Radiocarbon* **62**, 207-218, doi:10.1017/Rdc.2019.108 (2020).
406 Ya, M., Wu, Y., Wang, X., Li, Y. & Su, G. The importance of compound-specific radiocarbon analysis in source identification of polycyclic aromatic hydrocarbons: A critical review. *Critical Reviews in Environmental Science and Technology*, 1-42 (2020).
407 Hendriks, L. *et al.* The Ins and Outs of C-14 Dating Lead White Paint for Artworks Application. *Analytical Chemistry* **92**, 7674-7682, doi:10.1021/acs.analchem.0c00530 (2020).
408 Beck, L. *et al.* Thermal decomposition of lead white for radiocarbon dating of paintings. *Radiocarbon* **61**, 1345-1356 (2019).
409 Toffolo, M. B. *et al.* Structural Characterization and Thermal Decomposition of Lime Binders Allow Accurate Radiocarbon Age Determinations of Aerial Lime Plaster. *Radiocarbon* **62**, 633-655, doi:10.1017/RDC.2020.39 (2020).
410 McGeehin, J. *et al.* Stepped-combustion C-14 dating of sediment: A comparison with established techniques. *Radiocarbon* **43**, 255-261 (2001).
411 Hajdas, I., Maurer, M. & Röttig, M. B. Development of 14C Dating of Mortars at ETH Zurich. *Radiocarbon* **62**, 591-600, doi:10.1017/RDC.2020.40 (2020).
412 Hua, Q. *et al.* Progress in radiocarbon target preparation at the ANTARES AMS Centre. *Radiocarbon* **43**, 275-282 (2001).
413 Aerts-Bijma, A. T., van der Plicht, J. & Meijer, H. Automatic AMS sample combustion and CO2 collection. *Radiocarbon* **43**, 293-298 (2001).
414 Nemec, M., Wacker, L. & Gaggeler, H. Optimization of the Graphitization Process at Age-1. *Radiocarbon* **52**, 1380-1393 (2010).
415 Salazar, G., Zhang, Y., Agrios, K. & Szidat, S. Development of a method for fast and automatic radiocarbon measurement of aerosol samples by online coupling of an elemental analyzer with

a MICADAS AMS. *Nuclear Instruments and Methods in Physics Research Section B: Beam Interactions with Materials and Atoms* **361**, 163-167 (2015).
416 Steier, P. *et al.* A new UV oxidation setup for small radiocarbon samples in solution. *Radiocarbon* **55**, 373-382 (2013).
417 Murseli, S. *et al.* The preparation of water (DIC, DOC) and gas (CO2, CH4) samples for radiocarbon analysis at AEL-AMS, Ottawa, Canada. *Radiocarbon* **61**, 1563-1571 (2019).
418 Burr, G. S., Edwards, R. L., Donahue, D. J., Druffel, E. R. M. & Taylor, F. W. Mass-Spectrometric C-14 and U-Th Measurements in Coral. *Radiocarbon* **34**, 611-618 (1992).
419 Wacker, L., Fulop, R., Hajdas, I., Molnar, M. & Rethemeyer, J. A novel approach to process carbonate samples for radiocarbon measurements with helium carrier gas. *Nuclear Instruments & Methods in Physics Research Section B-Beam Interactions With Materials and Atoms* **294**, 214-217, doi:10.1016/j.nimb.2012.08.030 (2013).
420 Garnett, M. & Murray, C. Processing of CO2 samples collected using zeolite molecular sieve for 14C analysis at the NERC Radiocarbon Facility (East Kilbride, UK). *Radiocarbon* **55**, 410-415 (2013).
421 Gaudinski, J. B., Trumbore, S. E., Davidson, E. A. & Zheng, S. Soil carbon cycling in a temperate forest: radiocarbon-based estimates of residence times, sequestration rates and partitioning of fluxes. *Biogeochemistry* **51**, 33-69 (2000).
422 Russ, J., Hyman, M., Shafer, H. J. & Rowe, M. W. Radiocarbon dating of prehistoric rock paintings by selective oxidation of organic carbon. *Nature* **348**, 710-711 (1990).
423 Rowe, M. *et al.* Application of supercritical carbon dioxide-co-solvent mixtures for removal of organic material from archeological artifacts for radiocarbon dating. *Journal of Supercritical Fluids* **79**, 314-323, doi:10.1016/j.supflu.2013.01.002 (2013).
424 Vogel, J. S., Southon, J. R., Nelson, D. E. & Brown, T. A. Performance of Catalytically Condensed Carbon for Use in Accelerator Mass-Spectrometry. *Nuclear Instruments & Methods in Physics Research Section B-Beam Interactions with Materials and Atoms* **233**, 289-293 (1984).
425 Wacker, L., Nemec, M. & Bourquin, J. A revolutionary graphitisation system: Fully automated, compact and simple. *Nuclear Instruments & Methods in Physics Research Section B-Beam Interactions with Materials and Atoms* **268**, 931-934 (2010).
426 Marzaioli, F. *et al.* Zinc reduction as an alternative method for AMS radiocarbon dating: Process optimization at CIRCE. *Radiocarbon* **50**, 139-149 (2008).
427 Xu, X. M., Gao, P. & Salamanca, E. G. Ultra Small-Mass Graphitization by Sealed Tube Zinc Reduction Method for Ams C-14 Measurements. *Radiocarbon* **55**, 608-616 (2013).
428 Rinyu, L., Orsovszki, G., Futo, I., Veres, M. & Molnar, M. Application of zinc sealed tube graphitization on sub-milligram samples using EnvironMICADAS. *Nuclear Instruments & Methods in Physics Research Section B-Beam Interactions With Materials and Atoms* **361**, 406-413, doi:10.1016/j.nimb.2015.03.083 (2015).
429 Janovics, R., Futó, I. & Molnár, M. Sealed Tube Combustion Method with MnO 2 for AMS 14 C Measurement. *Radiocarbon* **60**, 1347-1355 (2018).
430 Siegenthaler, U., Heimann, M. & Oeschger, H. C-14 Variations Caused by Changes in the Global Carbon-Cycle. *Radiocarbon* **22**, 177-191 (1980).
431 Suess, H. E. Radiocarbon Concentration in Modern Wood. *Science* **122**, 415-417 (1955).
432 Levin, I., Kromer, B. & Hammer, S. Atmospheric Delta (CO2)-C-14 trend in Western European background air from 2000 to 2012. *Tellus Series B-Chemical and Physical Meteorology* **65**, doi:10.3402/tellusb.v65i0.20092 (2013).
433 Barisevičiūtė, R. *et al.* Distribution of radiocarbon in sediments of the cooling pond of RBMK type Ignalina Nuclear Power Plant in Lithuania. *PloS one* **15**, e0237605 (2020).
434 Rakowski, A. Z., Kuc, T., Naxamura, T. & Pazdur, A. Radiocarbon concentration in urban area. *Geochronometria: Journal on Methods & Applications of Absolute Chronology* **24** (2005).
435 Svetlik, I. *et al.* Radiocarbon in the air of central Europe: Long-term investigations. *Radiocarbon* **52**, 823-834 (2010).

436 Hancock, G. J., Tims, S. G., Fifield, L. K. & Webster, I. T. The release and persistence of radioactive anthropogenic nuclides. *Geological Society, London, Special Publications* **395**, SP395. 315 (2014).
437 Waters, C. N. *et al.* Can nuclear weapons fallout mark the beginning of the Anthropocene Epoch? *Bulletin of the Atomic Scientists* **71**, 46-57, doi:10.1177/0096340215581357 (2015).

Acknowledgements

The authors apologize to the authors of numerous papers that could not be cited owing to limited space. We acknowledge monumental contributions of generations of radiocarbon researchers and researchers using radiocarbon in this flourishing and exciting field. Comments from anonymous reviewers and discussions with numerous colleagues in the field were most helpful, much appreciated and improved this publication.

I.H. acknowledges support of her research by the Laboratory of Ion Beam Physics, ETH Zurich. Special thanks are for the laboratory technical support for their dedicated work. Numerous researchers from various disciplines and countries are thanked for fruitful collaborations.

P.A. and M.G. acknowledge the UK Natural Environment Research Council, through (NE/S011854/1; NEIF) and the Scottish Universities Environmental Research Centre (SUERC) for funding and support. They express their deep gratitude to colleagues at SUERC for stimulating discussion and ideas, providing dedicated technical support and fruitful academic collaborations. S.F. acknowledges support from the Research School of Earth Sciences, The Australian National University and R. Wood and R. Esmay for their dedication and support to the ANU Radiocarbon Laboratory. C.P. acknowledges support from the Malcolm H. Wiener Foundation, the University of Arizona and members of the IntCal Working Group. K.L.S. acknowledges support of her research from the Swedish Research Council (542-2013-8358), the Strategic Research Program for Diabetes at Karolinska Institutet (C5471152), the Novo Nordisk Foundation (NNF12OC1016064, NNF20OC0063944), Vallee Foundation Vallee Scholar Award (C5471234) and the Karolinska Institutet/Astra Zeneca Integrated Cardiometabolic Centre (H725701603). G.Q. express his profound gratitude to the colleagues of the Centre of Applied Physics, Dating and Diagnostics at the University of Salento for their friendship, continues support, restless and dedicated work. H.Y. and M.Y. wish to thank the Laboratory of Radiocarbon Dating team at the University Museum of the University of Tokyo for their

relentless effort to improve the precision and accuracy of radiocarbon dating together with field archaeologists and researchers in Japan and the world.

I.H. and G.Q. acknowledge the inspiration and stimulating discussions with the IAEA (International Atomic Energy Agency) staff and the colleagues within the Coordinated Research Projects: Enhancing Nuclear Analytical Techniques to Meet the Needs of Forensic Sciences.

Author contributions

Introduction (I.H., P.A., C.P. and G.Q.); Experimentation (I.H., P.A., M.H.G., C.P. and G.Q.); Results (I.H., P.A., M.H.G., C.P. and G.Q.); Applications (I.H., P.A., M.H.G., S.J.F., C.P., G.Q., K.L.S., H.Y. and M.Y.); Reproducibility and data deposition (I.H., P.A., M.H.G., C.P. and G.Q.); Limitations and optimizations (I.H., P.A., M.H.G., C.P., G.Q. and K.L.S.); Outlook (I.H., P.A., M.H.G., C.P., G.Q. and K.L.S.); Overview of the Primer (I.H.).

Competing interests

The authors declare no competing interests.

Peer review information

Nature Reviews XXX thanks [Referee#1 name], [Referee#2 name] and the other, anonymous, reviewer(s) for their contribution to the peer review of this work.

Related links

IAEA C-1: https://nucleus.iaea.org/sites/ReferenceMaterials/Pages/IAEA-C-1.aspx

CALIBomb: http://calib.org/CALIBomb/

IntCal data: http://intcal.org/

ORAU: https://c14.arch.ox.ac.uk/databases.html

Gliwice Radiocarbon Laboratory: http://www.carbon14.pl/IB_Grdb/index.html

^{14}CARHU: https://www.oasisnorth.org/carhu.html

Royal Institute for Cultural Heritage: http://c14.kikirpa.be/search.php

New Zealand Radiocarbon Database: https://www.waikato.ac.nz/nzcd/

Supplementary information

Supplementary information is available for this paper at https://doi.org/10.1038/s415XX-XXX-XXXX-X

Figure legends

Figure 1. The **life cycle of ^{14}C** (A) Highly energetic charged particles from outer space called cosmic rays — mainly protons — create cascades of particles when interacting with nuclei of the atmosphere. (B) Neutrons liberated in these reactions enter the nucleus of atmospheric ^{14}N, knocking out a proton. (C)

The net result is that ^{14}N (7p+7n) is transformed into ^{14}C (8n+6p) with the addition of one neutron and loss of one proton. (D) The nuclei of ^{14}C are radioactive and decay with a half-life of 5700 ± 30 years[6]. This half-life differs from the Libby half-life value of 5568 ± 30 years[363] as well as from the Cambridge half-life of 5730 ± 40 years[364]. Radiocarbon ages are calculated using the Libby half-life, and are therefore not affected by the change in $T_{1/2}$. The mean lifetime of ^{14}C is around 8223 years. (E) Spontaneous ejection of an electron and an anti-neutrino in ^{14}C decay results in the atom once again becoming ^{14}N.

Figure 2. **AMS ^{14}C analysis process**. Samples are pre-treated according to requirements based on the sample, site and application. The purified material is transformed to CO_2 by oxidation, thermal decomposition or hydrolysis, depending on sample type. The CO_2 obtained from milligram-sized samples is then either graphitized or transferred directly into the sputtering ion source of the AMS system, when smaller i.e., µg-sized. The negative ion beam of carbon passes through various filters to remove isobaric interferences. In this process, electrostatic analyzers (ESA) bend the ions' trajectories depending on their energy-to-charge ratio. Magnetic elements (magnets I and II) separate ions depending on their magnetic rigidity, which are dependent on mass and velocity. Magnet I separates mass 12, 13, and 14 amu beams, which are sequentially injected into the high-voltage stage. Here, unwanted molecular isobaric interferences such as $^{12}CH^-$, $^{12}CH^{2-}$ and $^{13}CH^-$ are broken in collisions with a low-density gas, called the stripper. In this process they lose electrons and charge exchange to positive ions which are further accelerated. In the high-energy spectrometer, magnet II separates molecular fragments from the required radiocarbon and the stable carbon isotopes. The latter are measured as ion currents in a Faraday cup. The second ESA is used to further filter atomic ions of mass 14 amu, allowing the detection of ^{14}C by single ion-detecting techniques: either gas-filled ionization chambers or semiconductor detectors. Obtained isotope ratios are compared to those of reference materials analyzed under the same measurement conditions to calculate $F^{14}C$ and radiocarbon age.

Figure 3. Calibration curve and precision of calendar ages. Known-age samples such as calendar dated tree-rings extending back to 13,900 calendar age counted backwards from 1950 CE (cal BP) or other independently-dated records such as from speleothems, lake sediments, corals and stalagmites[8] are used to generate radiocarbon measurements in radiocarbon years BP (where 0 BP = 1950 CE) for calibration**.** (A) The INTCAL20[8] calibration

curve for the terrestrial Northern Hemisphere. Radiocarbon years BP / $\Delta^{14}C$ are plotted on the Y axis, the calibrated date equivalent is plotted along the X axis in either cal BP (calendar ages counted backwards from 1950 CE), AD/CE or BC/BCE. The visible offset between radiocarbon time scale and the calendar time scale (1:1 between time scales is shown as dashed line) is due to calculated radiocarbon age using an underestimated half-life and due to the variable atmospheric ^{14}C content. Conversion of radiocarbon years BP to $\Delta^{14}C$ provides a more direct record of increases and decreases in atmospheric ^{14}C through time by removing fractionation effects. When $\Delta^{14}C$ is increasing slopes are produced in the calibration curve, when it is decreasing plateaus occur. (B) Calibration and the effects of curve shape. Hypothetical radiocarbon measurements of a textile, skull and charred seeds with equal uncertainly 1σ. Horizontal lines from the measured radiocarbon age (RA) + 2σ and RA - 2σ intersect with the calibration curve. At the point of intersection, the calibrated age can be read on the X-axis as calendar age, either AD/CE or BC/BCE. Measurements for the textile correspond to a period of increasing $\Delta^{14}C$ (beige line), resulting in a precise date range (green). The age of skull corresponds to a period of decreasing $\Delta^{14}C$, yielding a less precise range (purple). The radiocarbon age of the charred seeds intersects the curve during a period of more frequent changes in $\Delta^{14}C$, which produce multi-modal probability distributions (yellow). (C) Output plots of calibration. The pair of darker blue curves demarks the calibration curve and the shaded blue area between represents its uncertainly (plus and minus one standard deviation), the red curve on the left indicates the radiocarbon concentration in the sample. The gray histograms show the range of possible ages for the samples at 2σ level or 95.4 % confidence level shown as ranges below histograms. (Ca) The radiocarbon age of the textile is 2600 ± 20 BP calibrates to the slope preceding the plateau, resulting in calendar age between 806 and 776 BCE. (Cb) The age of 2460 ± 20BP for the skull corresponds to the plateau, resulting in a wide age interval between 755 and 420 BCE. (Cc) The radiocarbon age of the charred seeds is 2160 ± 20 BP, which calibrates to two distinct intervals: 352—287 BCE and 228–219 and 211–109 BCE.

Figure 4 Calibration of radiocarbon ages. Examples of calibration using the OxCal calibration software[98]. (a) Samples with $F^{14}C < 1$ (positive radiocarbon age — 4b) are calibrated with IntCal20 data[8], while samples with $F^{14}C > 1$ (negative radiocarbon age — 4c) are calibrated with bomb peak data[101]. (b) A medieval age of 700 ± 20 BP is calibrated with IntCal20 data, as an example of positive radiocarbon age. The resulting calendar age encompasses two intervals:

1274–1303 CE and 1368–1380 CE (95.4% confidence level). (c) On a sample with $F^{14}C = 1.5 \pm 0.003$ (negative radiocarbon age), the bomb peak is used for calibration. Due to the rising and declining features of the bomb peak the measured value corresponds to two calendar time intervals: year 1963 CE and 1970–1972 CE.

Figure 5. Bayesian Modelling in radiocarbon dating. (a) The Bayesian approach to ^{14}C data analysis is an iterative process where, once obtained, the posterior distribution is checked to be statistically consistent with the set of data and the prior information[103,365] . When this agreement is not satisfactory a refinement of the model or the identification of possible outliers in the data are needed; **t** is the set of parameters, **d** the data or measurements made and P(**t**) is the prior or the information available about the parameters independent of the measurements. P(d|t) is the likelihood that d is true given that t is true. P(t|d) is also a conditional probability, that t is true given that d is true. P(t|d) is the posterior probability, given the measurements and the prior. (b) Example of a prior: Deposited material events ($Sopp_i$) occurred in a certain sequence over time (t_i), one after the other ($t_i < t_{i+1}$) , which is defined by a certain order ($Depth_i < Depth_{i+1}$). Input of ^{14}C ages obtained for a sequence of samples in sediment core using the OxCal model [98,366] provides (c) a model of the age-depth relationship of calibrated ages for the $Sopp_i$ samples (5b). d) The probability distribution of a typical calibration if radiocarbon age (red curve) is shown as a light grey curve on the X-axis. As a result of the model, some regions of calendar ages are excluded resulting in higher precision of calendar age, represented by the dark grey curve on the X-axis. Agreement Index is an indicator of the match between the data and the model.

Figure 6. Radiocarbon dating of sedimentary records. Terrestrial or marine sediments, soils and peat sections can provide information about chronology and carbon sources. (a) Sampling of bulk sediments is followed by sieving so that different fractions can provide different information. (b) Macro remains (terrestrial) or hand-picked foraminifera shells (marine) are subjected to radiocarbon dating analysis. The resulting radiocarbon ages of terrestrial macro remains or foraminifera are used to construct age-depth model. Radiocarbon ages of total organic carbon (fine fraction < 150 µm to remove roots)[367] can be compared with terrestrial macrofossils for evaluation of reservoir ages. (c) Chromatographic separation of biomarkers for radiocarbon dating (CSRA)[63,368] allows tracing different sources and processes such as mobilization and transport of old carbon stored in soils. The increasing offset of radiocarbon ages measured of the long chain n-alkanes (C_{27}–C_{31}) was observed in the top 300 cm of

well-dated sedimentary records from Soppensee[105]. The change occurred around 4,000 years BP following the first human occupation in the region at around 4,500 years BP[369].

Figure 7. Distribution of ^{14}C in human body. The bomb peak provides a unique opportunity for biomedical studies to measure cell formation and turnover rates in the human body. (a) Carbon is obtained from dietary sources and integrated into human tissues. With the exception of fish and other aquatic organisms, dietary sources reflect the ^{14}C content of the atmosphere. Depending on the tissue's turnaround time, the ^{14}C concentration measured in different sources and tissues will differ. (b) $F^{14}C$ measured in various tissues and organs from a person born in 1965 show that eye lens proteins[300,301] and neurons from the cerebral cortex[248] retain carbon corresponding to the year of the birth. Tooth enamel does not turnover carbon after the completion of enamel formation, allowing it to be used forensically to determine the date of birth of an individual[297]. $F^{14}C$ analyses in other organs provide insight to the dynamics of cell and tissue formation and turnover rates, like the renewal of cardiomyocytes in the heart muscle decreases with age[254], and the formation of cartilage and Achilles tendon is completed before adulthood[370,371]. The $F^{14}C$ in fat cells, blood, nails, hair, skin collagen and bone lipids, which are constantly renewing, is in equilibrium with the diet's ^{14}C signature [256 372].

Fig. 8. ^{14}C analysis of cultural heritage items and detection of forgeries. (a) Examples of objects that can be analyzed. Paintings are often analyzed, while musical instruments are not common, but here represent all wooden objects**.** (b) Fragments of materials such as paint (lead white), canvas or wood are inspected under a stereomicroscope, and analysed using arrange of techniques including FTIR[274,275], Raman spectroscopy[373,374], XRF[276], XRD[375], GC-MS [277-280] to assist in the formulation of appropriate research questions and sampling strategies. Ethical guidelines of sampling and dating cultural heritage items must be observed[71-73] (c) Two radiocarbon dates measured on the paint (Ca) and canvas (Cb) imply a case of a forgery: as indicated by the $F^{14}C > 1$ obtained from the binding media in the paint[326], whereas the canvas (Radiocarbon age: 150 ± 20 years BP) dates to time between 1669 and 1950 CE (95.4% confidence level). The radiocarbon dating of a canvas from this period is an example of the problem caused by Stradivarius plateau[51]. (Cc) The radiocarbon dating of the wood sample (radiocarbon age: 250 ± 20 years BP) is also affected: three age intervals are possible between 1529 and 1799 CE (95.4% confidence level). Precision would be improved by dating a sequence of samples.

Boxes

BOX 1: Radiocarbon dating

Activity:

$A=\lambda N$ the number of disintegrations per time unit, proportional to the number of nuclei N and λ the decay constant

Measurements of ^{14}C activity:

Beta-counting: electrons released by ^{14}C using GPC or LSC

Accelerator Mass Spectrometry (AMS): ^{14}C atoms, $^{14}C/^{12}C$ ratio

Libby's Radiocarbon Age:

After t years from the formation of material, the sample's ^{14}C activity is A, which is proportional to the number of nuclei and the decay constant.

Elapsed time can be measured from the moment of death or deposition:

$t= -8033 \ln (A/A_0)$

A = radiocarbon activity at the time of dating

A_0 = initial radiocarbon activity at the time t_0 (deposition, formation, death)

$T_{[1/2]Libby} / \ln 2 = 8033$ years, where $T_{[1/2]Libby} = 5568$ years — the Libby half-life

Radiocarbon Age$= -8033 \ln F^{14}C$

$F^{14}C = A_{Sample}/A_{Standard}$

Activity ratio of the measured sample relative to reference material (95% of the activity of HOx1 in year 1950 CE) normalized for $\delta^{13}C$ i.e., isotopic fractionation[16].

For a comprehensive summary of terminology and units used in radiocarbon dating see [16,20,21]

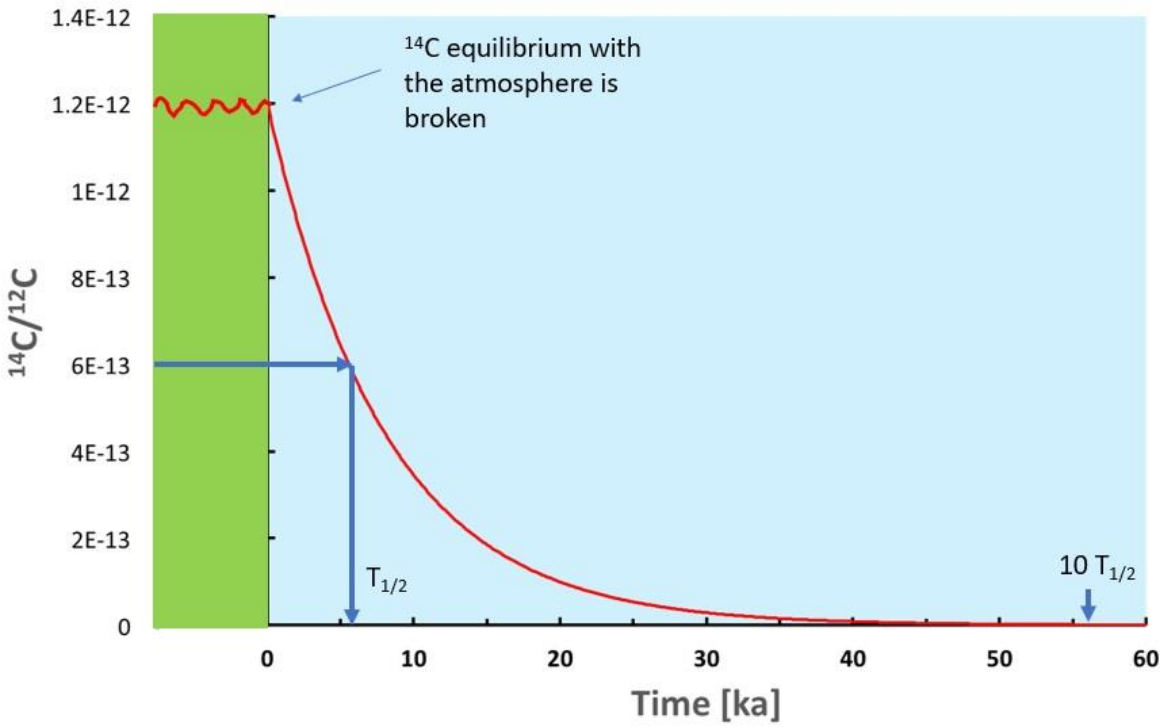

BOX 2 : ^{14}C sample Preparation

Step 1: Pre-screening and monitoring of sample purity

Aim: Investigation of the degree of purity and/or the preservation quality of the sample. This allows the most suitable analytical approach (step 2) to be chosen.

--**investigation** of the purity, preservation of material

Visual, UV light, polarized light microscopy, SEM[376,377]

Spectroscopy (IR[54,58,60,61,378-380], Raman[58,279,381-386] , XRF[279,387], XRD[279], X-Ray[388])

Pyrolysis–gas chromatography–mass spectrometry Py-GS-MS[57,389-394], thermal gravimetric analysis TGA[386], Nuclear magnetic resonance spectroscopy NMR[395]

%C and N [54,396]

Step 2: Isolation of carbon for measurement

Aim: Removal of carbon that is not of interest for measurement from the sample:

--**removal** of exogenous carbon

Physical (washing, ultrasonic baths, sieving, manual selection, removal of surface)[61,62]

Chemical (Acid, Base, solvents, oxidation, leaching with acid, bleach)[61,62,397]

--**selection** and extraction of endogenous carbon if a particular compound or compound class is required for measurement

Compound specific (cellulose[398-401], amino acids bones[120], biomarkers[44,63-66,402-406])

DNA[246]

Thermal decomposition (lead white[407,408], mortar[409])

Step combustion[397,410]

Sequential dissolution[411]

Step 3: Conversion of isolated sample carbon to CO_2 or elemental C for measurement

Aim: remove non-carbonaceous components of the sample prior to measurement and convert sample C into a form suitable for AMS measurement. If measurement is to be performed by liquid scintillation or gas proportional counting, this step involves conversion of sample C into a form suitable for these methods (e.g. C_6H_6 in the case of liquid scintillation counting)[25]

--**Conversion** of all carbonaceous compounds in the sample to CO_2

Combustion in Vycor tubes [412]

Combustion in EA[413-415]

ramped pyrolysis/oxidation[273,410]

UV-oxidation[416]

Wet-oxidation [45,417]

Acid hydrolysis [46,418,419]

Trapping CO_2 [420,421]

Laser Ablation [47,97]

Plasma[422,423]

Sample preparation may be complete after this stage, if the AMS measurement will involve a gas ion source

-- Conversion of the sample CO_2 to graphite following one of the methods above

H_2 &Co/ Fe catalyser[14,424,425]

Closed tubes Fe/Zn[426-428] and Mn[429]reduction

BOX 3: Variability of atmospheric ^{14}C

Incoming cosmic radiation leads to the production of neutrons which react with nitrogen to form ^{14}C in the upper atmosphere**.** This radiocarbon is quickly oxidized and mixed in the Earth's atmosphere. It enters the biosphere via photosynthesis and the food chain, and the hydrosphere via gas exchange. Atmospheric ^{14}C concentration fluctuates around 1.8×10^{-12} (by conventional pre-industrial levels). The various reservoirs of carbon have concentration equal to the atmosphere or lower in the deep ocean[430].

Production rate

Variable geomagnetic shielding[179], solar activity[361] and so called cosmic events[169-171] are the mechanisms behind changes in production of ^{14}C, which modulate the $(^{14}C/^{12}C)_{atm}$. In general, weak shielding translates into higher production rate and higher $(^{14}C/^{12}C)_{atm}$.

Global Carbon Cycle

The ocean is the largest of the carbon pools[430] with a long turnover time (~2,000 years), therefore changes in ocean circulation have an impact on the $(^{14}C/^{12}C)_{atm}$. Other reservoirs such as soil, peat, permafrost and sediments, which have capacity to store carbon can be sources of old carbon, and therefore have an impact on the $(^{14}C/^{12}C)_{atm}$.

Anthropogenic Effects

Following Industrialization the combustion of fossil fuels has lowered the $(^{14}C/^{12}C)_{atm}$. This anthropogenic effect was first observed by H. Suess in tree-rings[431]. The impact of the Suess effect has been obscured by artificial production of ^{14}C in the nuclear tests of 1952–1963 when atmospheric $F^{14}C$ was doubled[101,432] and ^{14}C signal was also transferred into the other reservoirs. However, as the combustion of fossil fuels continues the Suess effect is again becoming the prevailing anthropogenic effect[197]. Increasingly, radiocarbon analysis performed in any type of archive functions as a tracer of anthropogenic activity [433-435].

BOX 4: Bomb peak ^{14}C

The development and testing of powerful hydrogen bombs in 1952 led to the fallout of radionuclides[436], and affected $(^{14}C/^{12}C)_{atm}$, known as the bomb peak. The ^{14}C bomb peak effect is observed as an excess in ^{14}C concentration (above natural level) and measured in material that was formed between 1954 and current year. Following the Nuclear Ban Treaty in 1963 the excess levels of ^{14}C decreased with transfer to other reservoirs, mainly oceans, and the (Suess effect)[431]. The distribution of bomb ^{14}C around the globe is not uniform and requires the compilation of data sets for different geographic regions [101]. The signal of artificial ^{14}C provides a unique geochronological tool[437] as well as an environmental tracer as the atmospheric $^{14}CO_2$ marked by bomb ^{14}C is exchanged between carbon reservoirs. Bomb peak analysis is used to study ocean circulation, human tissue turnover time, forensic anthropology, transport and storage of carbon between carbon pools, detection of forgeries, illegal wildlife products trade, aging of fish and annual tree-ring growth. Because of the Suess effect and decreasing $(^{14}C/^{12}C)_{atm}$ [197] bomb peak radiocarbon dating will require the support of other methods such as the use of stable carbon isotopes[310]

BOX 5: Requirements and checks for dating of biological samples

Prior to deciding whether to use radiocarbon dating, it is important to determine whether the cell type of interest can be isolated with close to 100% purity, and whether enough cells will be obtained for radiocarbon dating.

To date genomic DNA to determine cell age and turnover, with current AMS limitations regarding sample size, a minimum of 5×10^6 cells is needed, assuming that one-third of DNA is carbon and a normal diploid cell contains approximately 6 picograms of carbon. This cell yield is not possible for all biological structures.

If yield and purity are possible, then specific DNA extraction protocols have been developed to avoid contaminating the DNA sample with exogenous carbon[246,250,255,256]. Petroleum-derived carbon sources may introduce trace amounts of ^{14}C-depleted carbon into the sample, depressing ^{14}C values and resulting in false age estimates. Similarly, RNA, protein or lipid contamination will also impact results, introducing non-DNA sources of carbon. Trace amounts of contamination in large samples can be tolerated without too much impact on age estimates, however when working with DNA to determine cell age, samples are rarely large and small sources of contamination can significantly impact results and age estimates.

Stringent checks should be put in place, including assessing samples for DNA purity, as well as measuring the amount of DNA in the sample to be measured and comparing against the amount of carbon measured, which can indicate contamination with non-DNA sources of carbon. Control DNA samples of known age are good reference samples to be included in each test run.

Glossary

Global carbon cycle: Exchanges of carbon between carbon reservoirs, including the atmosphere, biosphere, oceans and sedimentary deposits.

Radiocarbon calibration curves: Experimental reconstruction of past atmospheric ^{14}C recorded in tree-rings and other independently dated samples like speleothems, marine corals and laminated sediments.

Isobar: atoms of different elements or molecules with the same atomic mass

Archives: natural records of information about the past environment such as; sediments, soils, peat bogs, cave deposits, corals and tree-rings

Reservoir effect: an apparent age of material due to mixed carbon sources when old carbon is added to atmospheric CO_2.

Isotope fractionation: enrichment of one isotope relative to another due to chemical reactions or physical processes

Activity ratio:

Constant mass contamination correction: mass and ^{14}C signature of contamination as evaluated for specific preparation process to correct for exogenous carbon introduced to samples containing tens of micrograms of carbon.

Marine radiocarbon reservoir effect: an offset in ^{14}C age between contemporaneous organisms from the terrestrial environment and organisms that derive their carbon from the marine environment.

Freshwater reservoir effect: anomalously old radiocarbon ages of samples from lakes and rivers due to water rich in dissolved ^{14}C-free calcium carbonates.

Dead carbon fraction: the amount of radioactively dead carbon that reduces the ^{14}C content in speleothems.

Diagenesis: combination of physical, chemical and biological processes that occur in a sample after the deposit.

Compound-specific radiocarbon analysis: radiocarbon analysis of individual organic compounds (biomarkers) such as lipids, fatty acids, proteins and waxes of a specific molecular size after chromatographic separation

Phytoliths: silica structures formed in plant tissues by the uptake and storage of silica from soil, which occlude and preserve organic carbon

Proxy data: data gathered from natural archives of climate variability, such as tree-rings, ice cores, fossil pollen, ocean sediments, coral and historical data.

Solar energetic particles: high-energy particles protons, electrons and high-energy nuclei coming from the sun.

Mycorrhizal symbiosis: exchange of photosynthesized carbon for mineral nutrients obtained by mycorrhizal fungi

Saprotroph: organism that feeds on nonliving organic matter and has ability to decompose

Ventilation: the amount of time since a water particle last interacted with the atmosphere

Curve of Knowns: the first radiocarbon ages of well-dated historic items and wood published in 1949 by Arnold and Libby, proving the principle of the method

Vinci and Stradivarius age plateau: time periods 1450 – 1650 CE and 1700 – 1950 CE marked by nearly constant radiocarbon ages where calibrated ages result in multiple intervals

Bayesian wiggle-matching: calibration of a sequence of radiocarbon ages with a known time gap between them such as number of tree-rings.